A SYSTEM FOR CONTINUOUS SAMPLING OF BIOAEROSOLS GENERATED BY A POSTAL SORTING MACHINE

A Thesis

by

MATHEWS SEARS RICHARDSON

Submitted to the Office of Graduate Studies of
Texas A&M University
in partial fulfillment of the requirements for the degree of

MASTER OF SCIENCE

August 2003

Major Subject: Mechanical Engineering

A SYSTEM FOR CONTINUOUS SAMPLING OF BIOAEROSOLS GENERATED BY A POSTAL SORTING MACHINE

A Thesis

by

MATHEWS SEARS RICHARDSON

Submitted to Texas A&M University
in partial fulfillment of the requirements
for the degree of

MASTER OF SCIENCE

Approved as to style and content by:

Andrew McFarland (Chair of Committee)	William Marlow (Member)
Dennis O'Neal (Member)	Dennis O'Neal (Head of Department)

August 2003

Major Subject: Mechanical Engineering

ABSTRACT

A System for Continuous Sampling of Bioaerosols Generated
by a Postal Sorting Machine. (August 2003)
Mathews Sears Richardson, B.S., University of Texas, Austin
Chair of Advisory Committee: Dr. Andrew McFarland

In this study, a system for the collection of bioaerosols emitted from the mail sorting process was designed and characterized. Two different wetted-wall cyclones, the JBPDS cyclone and the glass cyclone sampler (GCS), were evaluated as system collection devices. These devices operate at 780 L/min and have a D_{50} of $\sim$1 μm. A trimming impactor with a D_{50} of 10 μm was used upstream of the collection devices. Using two reference probes, the cyclone liquid outputs were compared with aerosol collected on filters and the output of an Aerosol-to-Hydrosol Transfer Stage (AHTS).

The mass emission rate of the postal sorting machine was 3.15 mg/min and found not to vary significantly with flow rates above 700 L/min. On average, greater than 66% of the mass collected had a $D_a < 10$ μm. Using a Coulter Counter, the volume median diameter (volume equivalent) for both device hydrosol outputs was 4.18 μm. For the effluent aerosol, the volume median diameter was 12.5 μm.

For a bioaerosol release, this study found that greater than 65% (by volume) of the material released had a D_a greater than 7.2 μm. Using filters, it was found that on average, 95% of the bioaerosol particles emitted had a D_a less than 10 μm. According to the reference data, the expected number of bioaerosol particles in 1.5 times that collected by the GCS and 5.5 times that collected by the JBPDS cyclone for a one milligram release. The time constant for the system in response to a letter release was found to be 1.3 minutes for the GCS and 1.75 minutes for the JBPDS cyclone.

A final note to this study states that the probe dimensions were incorrectly developed, therefore affecting the aspiration efficiency of the probes. In turn, this may have affected the outcome of some of the results. A plot is given at the end of the paper showing to what extent the results may have been effected. It is recommended that further experimental studies be performed to verify the results in this study.

For my wife, Sasha, who makes life sweet.

ACKNOWLEDGMENTS

I would like to acknowledge the contribution and support of the following people:

Dr. Andrew McFarland, my advisor and committee chair, who provided the ideas, support and encouragement that made this project interesting and fun to work on.

Dr. William Marlow and Dr. Dennis O'Neal, my remaining committee members, who took the time to be on my committee and support me.

Those at Siemens Dematic who provided financial and physical support, including: Mark Koreneck, who has enthusiastically supported the development of this system for the past year; Jim Amigh, who turned our drawings into pieces of a functioning system; Mike Yaklin, whose knowledge of controls and software has helped make the collection system manageable; all others who in some way or another contributed support.

Those at CTC who put their time, effort, and money into the development of a detector, including: Tammy Santanna, who answered many questions concerning the fundamentals of the detectors and provided much needed microbiological analytic support; Tim Postlethwaite, who made several trips down to College Station to oversee integration efforts for the detector and collection system.

Carlos Ortiz, who contributed much time and energy to the development of the collection system; John Haglund, who got this project off of the ground and provided support and insight; Denis Phares, who provided insight and ideas concerning the analysis of aerosol data.

Kim Dubose in the clinical microbiology lab in the veterinary medical hospital, who took time out of her day to talk with me about biological contamination.

My wife, Sasha Richardson, who took the time to look over this paper and ensure that it was readable and coherent. She also provided valuable advice in the analysis of microbiological samples.

To all members of the ATL, past and present, who took the time to move mail, run analysis or tests, generate beautiful drawings or just listen to me, including: Tina Famighetti, Ginny Wisnit, Travis Owens, Brandon Dooley, Brandon Moncla, Youngjin Seo, Vishnu Vijayaraghvan , Hammad Irshad, Nagaraj Ramakrishna, and Amit Gupta.

TABLE OF CONTENTS

Page

LIST OF TABLES

LIST OF FIGURES

NOMENCLATURE, ABBREVIATIONS, AND UNITS

Nomenclature

A_2	venturi meter throat cross-sectional area
A_i	cyclone inlet area
A_j	impactor jet cross sectional area
α	significance level for statistical tests
b	base of a rectangle
β	logistic slope parameter
C_c	slip correction factor
C_f	flow coefficient for the venturi meter
C_{in}	concentration of aerosol in the incoming gas stream
C_{i,SF_6}	SF_6 concentration in the incoming flow
C_{out}	concentration of aerosol in the exhaust gas stream
C_{s,SF_6}	SF_6 concentration in the system
D_a	aerodynamic diameter
D_c	cyclone body diameter
D_e	volume equivalent diameter
D_j	impactor jet diameter
D_{mm}	mass median diameter
D_{nm}	number median diameter
D_o	outlet diameter of a cyclone
D_p	particle diameter
D_{50}	cutpoint of a device

DF	dilution factor
ρ	gas density
ρ_o	unit density, 1000 kg/m^3
ρ_p	particle density
h	length of side
H_o	the null hypothesis
$\dot{m}$	mass emission rate
Δm_f	differential mass collected on a filter
N	number of colonies
$\bar{n}$	average number of colonies counted
η_a	aspiration efficiency
η_c	collection efficiency
η_p	penetration efficiency of a collection device
Q_p	reference flow rate
Q_s	system flow rate in L/min
Q_{SF_6}	SF_6 flow rate in mL/min
p	probability that H_o is true
ΔP_{vm}	differential pressure across the venturi meter
Re	Reynolds number
Re_f	Reynolds flow number
Stk	Stoke's number
Stk_{50}	Stokes number for particle with D_p equal to D_{50}
σ_g	geometric standard deviation
t_s	sampling time
tau	response time

U_i	inlet velocity
u_o	free-stream velocity (as defined within a probe shroud)
μ	gas viscocity
μ_s	population mean
V_o	initial volume
V_p	plated volume
W	characteristic dimension in the flow
χ	particle shape factor

Abbreviations

ABS	array bio-sensor
AHTS	Aerosol-to-Hydrosol Transfer Stage
ARL	Army Research Laboratories
ATL	Aerosol Technology Laboratory
ANOVA	analysis of variance
BG	*Bacillus globigii*
CDC	Centers for Disease Control and Prevention
COV	coefficient of variation
GCS	glass cyclone sampler
CFU	colony forming unit
COV	coefficient of variation
DBCS	Delivery Bar Code Sorter
DPA	dipicolinic acid
FCS	flow-cell system
GCS	Glass Cyclone Sampler

JBPDS	Joint Biological Point Detection System
PHC	positive-hole correlation
PM	particulate matter
PM-10	particulate matter with $D_a < 10$ μm
SEM	scanning electron microscope
SF_6	sulfur hexafluoride
TAMU	Texas A&M University
TSA	tryptic soy agar
USPO	United States Post Office
v/v	volume ratio

Units

CFU	Colony Forming Unit
kg/m^3	kilograms per cubic meter
kPa	kilopascals
L/min	liters per minute
m	meter
mm	millimeter
mg	milligrams
m/s	meters per second
mg/min	milligrams per minute
mL	milliliter
mL/min	milliliter per minute
Pa	pascals
ppm	parts per million

μm	micrometer, or micron

INTRODUCTION

In October of 2001, shortly after the attacks of September 11^{th}, the United States Post Office (USPO) found itself a victim of collateral damage caused by an unknown assailant disseminating *Bacillus anthracis* (also known as anthrax) through the mail. According to a report by the Centers for Disease Control and Prevention (the CDC), by the end of the fall of 2001, 22 cases of anthrax were suspected or confirmed (CDC 2001b). Between October 19^{th} and 21^{st} of that fall, there were a reported four postal workers from the Brentwood Mail Processing and Distribution Center in Washington, D.C. hospitalized with pulmonary, or inhalation, anthrax (CDC 2001a). Two of these employees eventually died.

Mail processing centers such as the Brentwood facility in Washington, D.C. contain machines similar to the Delivery Bar Code Sorter (DBCS), pictured in Figure 1, which process mail at high speeds. These machines accelerate mail to speeds as high as 14 m/s (CDC 2001a). A large amount of pressure is abruptly applied to envelopes as they are accelerated. At this point, material on or within the envelope may be unintentionally aerosolized. If an aerosolization event takes place, the machine and any mail in the proximity of the envelope will be contaminated.

The threat of aerosolizing bacteria is evident when reviewing studies performed by the CDC at the Brentwood mail facility. In one study, Dull et al. (2002) performed an analysis of the surface of the mail sorting machine after the anthrax events. In this study, performed after topical cleaning of the mail sorting machine using a 0.5% hypochlorite solution, samples from surfaces immediately around the feeder (where the envelopes are

---

The journal model is *Aerosol Science and Technology.*

Figure 1. Graphic of a delivery-bar code sorter (DBCS) with mail stackers. Courtesy of Siemens Dematic.

accelerated) contained anthrax colonies too numerous to count. Samples taken at other locations contained few colonies. Subsequent studies by Siemens Dematic, makers of the DBCS and other mail sorting machines, show that the area around the mail feeder is the primary point of potential aerosolization. Previous studies show that the threat of secondary aerosolization is insignificant relative to the primary event (CDC 2001a; Peters et al. 2002; Weis et al. 2002); this fact emphasizes the point that any collection system should sample at the primary point of aerosolization.

To prevent the tragedies such as that which occurred in the fall of 2001, Siemens Dematic has undertaken a program to develop a detection system that will provide a rapid response (within approximately three minutes) to the presence of anthrax. As part of the effort, Siemens Dematic contracted with the Aerosol Technology Laboratory (ATL) at Texas A&M University (TAMU) to develop a system to collect harmful material that may be emitted by a mail sorting machine. Samples collected using this system will be

delivered to another device for detection. Siemens Dematic has contracted with other organizations to develop detectors that will be integrated with the collection system.

At this time, Siemens Dematic is considering three detectors. In two of these devices, a fluorophore tagged antibody binds to a specific antigen (such as a protein unique to *B. anthracis*) which causes a visible reaction allowing the detection of the biological material. The other device is referred to as an endospore detection system (EDS) and uses 2,6-dicarboxypyridine (dipicolinic acid, or DPA) to identify bacteria in a sample. DPA is a chemical present in all endospores (Henis 1987).

The first of the antibody-antigen based system is termed the flow-cell system (FCS). Earlier tests indicated that the FCS might be able to detect 10^2 to 10^3 spores. As a point of reference, in the anthrax attacks on the USPO in 2001, spore concentrations for the spore powder were found to be $\sim 10^{12}$ spores/g (Peters et al. 2002). The second antibody-antigen system is the array-based biosensor (ABS). According to Golden et al. (2002), the ABS may be able to detect one to ten nanograms of biological material per one milliliter of fluid. Using the above concentration as a guideline, this may be roughly translated to about 10^3 to 10^4 spores. The EDS, an off-the-shelf technology (Ocean Optics, Inc., Dunedin, FL), claims a detection limit of 10^5 spores.

For the development and characterization of the collection system, Siemens Dematic provided a prototype of the DBCS to the ATL. This prototype resembles the DBCS in Figure 1, less the mail stackers. Siemens Dematic also provided undeliverable business mail for conducting the necessary background tests and simulating the release of biological material. The system for the collection of bioaerosols has been developed and this system has been characterized in terms of background emissions. The system has also been challenged with *Bacillus globigii*, or BG (also known as *B. subtilis v. niger*), to determine its collection characteristics in terms of bioaerosols. This collection system and the tests conducted for its characterization are described in this study. Preliminary integrated tests are currently being conducted to determine the collection characteristics of the total

collection-detection system.

SYSTEM DESIGN THEORY

Since June of 2002, several iterations of the sampling system have been developed and tested on the prototype DBCS. The latest iteration of the collection system described here is shown in Figure 2. In this system, a sample is extracted at the point of maximum potential aerosolization. This point was chosen based on data collected by the CDC and Siemens Dematic (CDC 2001a). The sample extraction point is located at the feeder, where mail is accelerated to 14 m/s. A set of perforated plates has been placed about the extraction point in order to act as a physical barrier to particles that may be released from an envelope (to prevent dispersion in unintended directions) and to maintain vacuum at the point of extraction. These plates reside in a large hood, which is sealed so that all of the flow is pulled through the plates. The vacuum created at the extraction point removes the particles from the boundary layer that might ordinarily travel with an envelope. A conceptual drawing showing the extraction point with and without plates is shown in

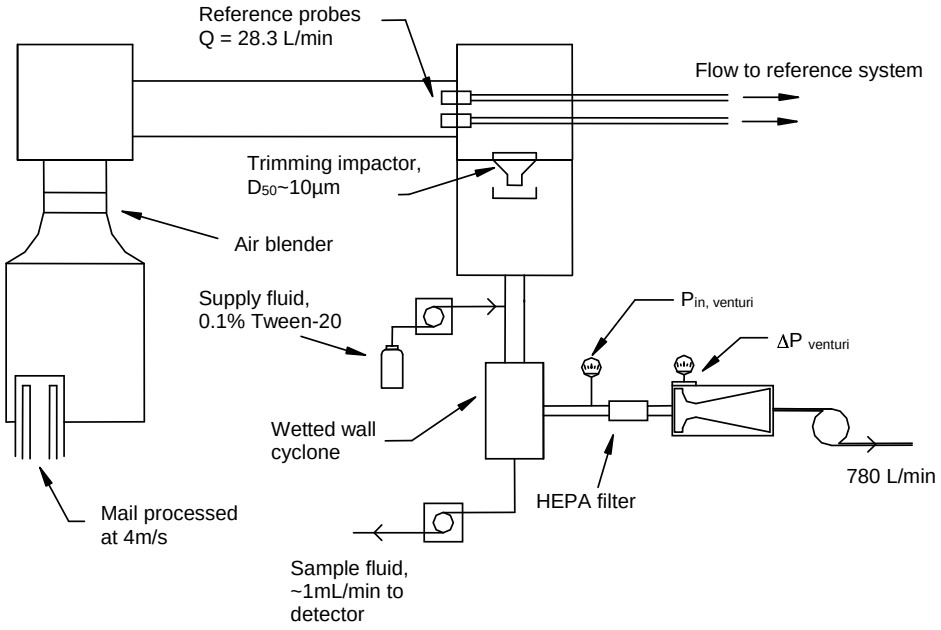

Figure 2. Schematic of collection system.

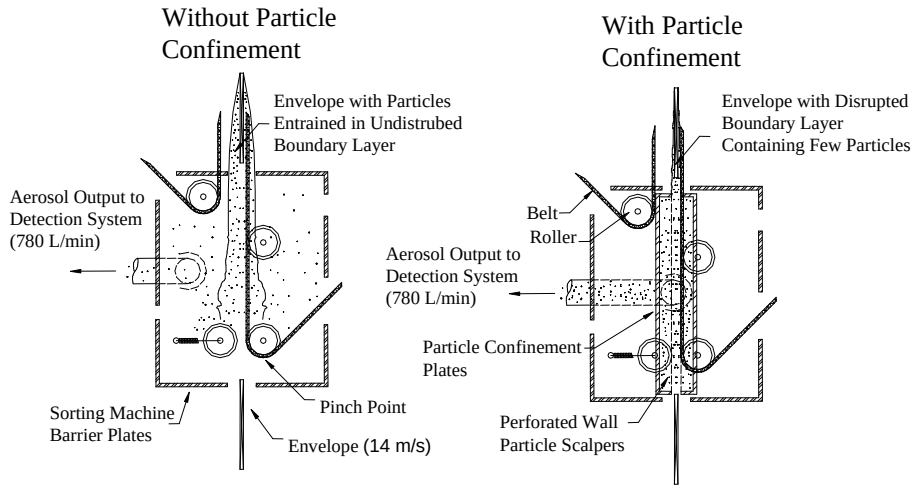

Figure 3. Conceptual drawing of the extraction point with and without the plates.

Figure 3.

An Air Blender (Blender Products, Inc., Denver, CO) is located immediately downstream of the extraction point. This is used to promote proper mixing of the sampled air. Immediately downstream of the Air Blender is a mixing plenum, 200 mm to a side. At this point, the flow is turned 90° and the box contracts to a duct, 100 mm×100 mm. The length of the duct is 0.91 m. Two reference probes are located near the outlet of this duct. The optimal length of the duct is based on the results of mixing tests performed by others at TAMU (Ortiz 2002). The results of those tests were used to determine where the probes should be placed so that they could extract a representative sample and were based on protocols outlined in the U.S. EPA Code of Federal Regulations (U.S. EPA 2003).

Collection of Reference Samples

The two reference probes located at the end of the duct are intended to be used to characterize the background emissions and biological releases from an envelope. These probes are shrouded probes designed to operate at 28.3 L/min based on data produced by Gong (1996). The shrouded probe was chosen over an isokinetic probe because the

wall losses are less. Also, the shrouded probe may be operated at a slightly off-angle and under subisokinetic conditions and still capture a representative sample (McFarland et al. 1989).

Following the probes is approximately 0.45 m of tubing with a diameter of 25.4 mm. One of the reference systems described in the following section are attached to the outlets of these two probes. Using the software *Deposition 2001a* developed in the ATL at TAMU (Riehl et al. 1996), the total penetration for an aerosol population can be calculated for a circular duct. Since the main duct in this system is square, the hydraulic diameter, D_h, must be used. The hydraulic diameter for a square duct is (White 1999, p. 358):

$$D_h = \frac{4\,b\,h}{2(b+h)} = h \qquad [1]$$

where h is the size of a side of the square duct. Using *Deposition 2001a*, the total penetration of particles with a log-normal distribution having a geometric mean diameter, D_{gm}, of 10 μm and a geometric standard deviation, σ_g, of 2 through the main duct is 95%. For the reference system (taking into account a bend required for the Anderson impactor), the total penetration of that same distribution through the reference system is 88%. At the outlet of the probes, the sampled air stream is processed as below; therefore, no deposition analysis was performed beyond this point for any aspect of the reference system.

The Aerosol-to-Hydrosol Transfer Stage

One reference used in this study was the Aerosol-to-Hydrosol Transfer Stage (AHTS) developed by Phan (2002) at TAMU. It operates on a principle similar to a standard inertial impactor. The AHTS samples air at a rate of 1 L/min and has 11 jets, each with a diameter of 0.25 mm. Given these dimensions, the cutpoint, D_{50}, of this device, based on the relations cited in Hinds (1999, p. 126), is 0.8 μm. The D_{50} of a device is defined as the diameter of particle for which all particles with size greater than D_{50} are captured

and all particles with size less than D_{50} pass through the device. This definition is for an ideal case with no internal wall losses of particles. In collection devices, the D_{50} is usually defined as the diameter for which collection efficiency is 50%. For a well designed impactor, such as the AHTS, the efficiency curve will approach a step function, as defined by the theory.

The AHTS differs from a traditional impactor in one aspect: the impaction surface is a liquid solution which flows through a sintered material. Based on Phan's data, the optimal solution is a 0.1% Tween-20 solution (v/v) (Fisher Scientific, Pittsburg, PA) with a flow rate of 0.5 mL/min. Griffiths et al. (1997) identified two different collection efficiencies for devices collecting particles in a wet medium. These are the penetration efficiency and the sampling efficiency. The penetration efficiency, η_p, can be found using the following equation:

$$\eta_p = 1 - \frac{C_{out}}{C_{in}} \qquad [2]$$

where C_{out} and C_{in} are the concentration of aerosol in the device outlet and inlet airstreams respectively. The penetration efficiency is the traditional device collection efficiency. The penetration efficiency of the AHTS is shown in Figure 4(a).

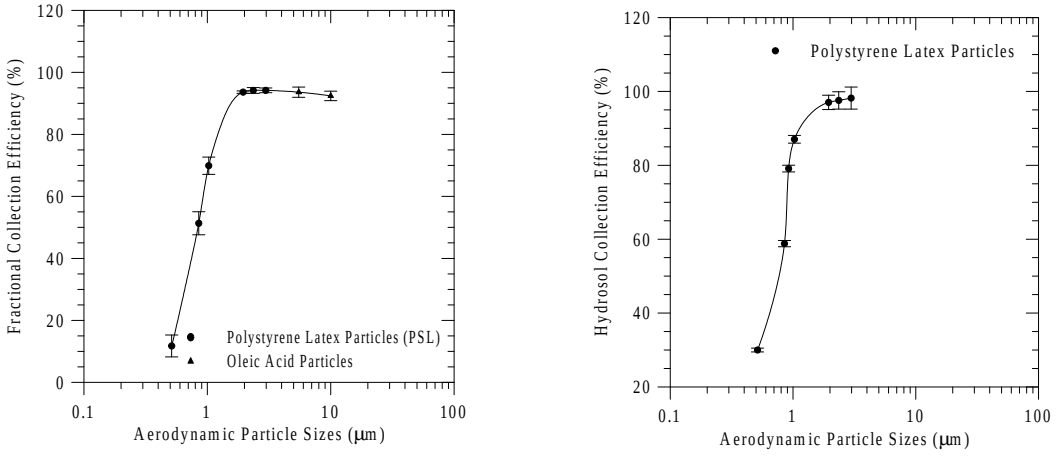

(a) (b)

Figure 4. Fractional efficiency curves for the AHTS as reported by Phan (2002). (a) Penetration efficiency and (b) collection efficiency.

The second collection efficiency of a device using a wet collection medium, the sampling efficiency, refers to the concentration of particles that are found in the sample fluid relative to the concentration of particles in the inlet airstream. As the particle size increases, the sampling efficiency will eventually begin to fall. This is because particles of greater size will encounter increasing difficulty penetrating the inlet of the device. In wetted-wall cyclones such as those used in this study, larger particles are more likely to be lost to the inlet walls. In the AHTS, the only limiting factor should be losses in the jet. The collection efficiency for the AHTS is shown in Figure 4(b).

The time constant for the AHTS, τ, is calculated as the time required for the hydrosol concentration to reach 63.2% of its steady state value in response to a step increase or decrease in the aerosol concentration. Phan found that τ for his test configuration was approximately 45 seconds. The results of system response time tests conducted by Phan are shown in Figure 5. In this figure, the recovery ratio is plotted against time. According

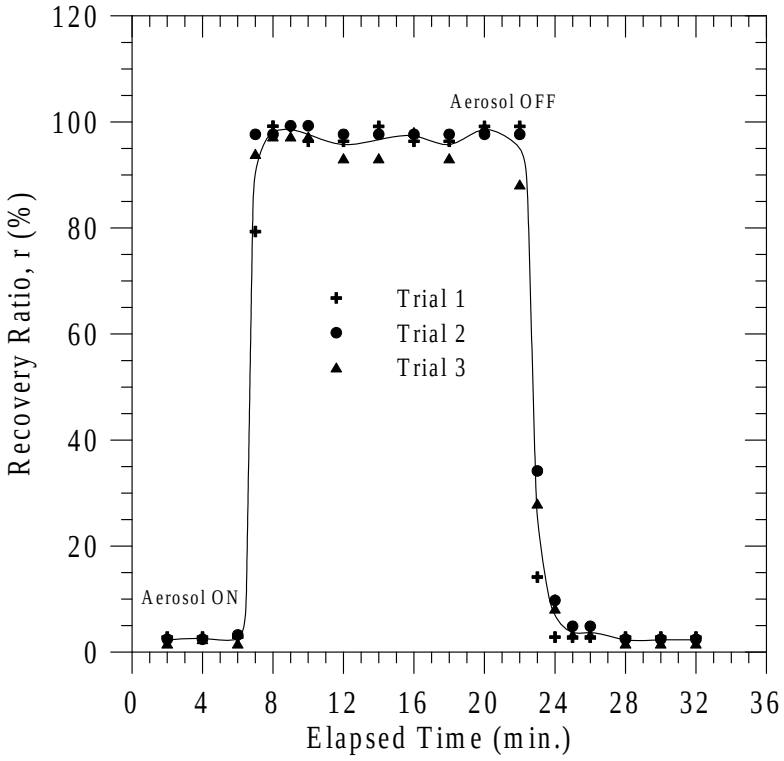

Figure 5. Results of system response time tests conducted by Phan (2002).

to Phan, the recovery ratio is the hydrosol particle collection rate over the total aerosol generation rate. In Figure 5, the aerosol generator was turned on in the sixth minute and turned off in the twenty second minute. It is necessary to note that the setup of a system may induce a lag in the response time (i.e. if fluid tubing is longer than that used in Phan's study).

The setup of the reference system for use of the AHTS is shown in Figure 6. In this figure, sampled air flows through the selected reference probe at 28.3 L/min. The flow is turned 90° and enters a flow splitter. The flow splitter is a tube which contains a plate near the bottom consisting of a series of holes arranged in radially symmetric pattern about a single, central hole. The outer holes create a sheath flow for the incoming gas to be sampled. The sheath air is exhausted from the system at 27.3 L/min through a capsule HEPA filter (Pall Gelman Sciences, Ann Arbor, MI). The remaining 1 L/min of

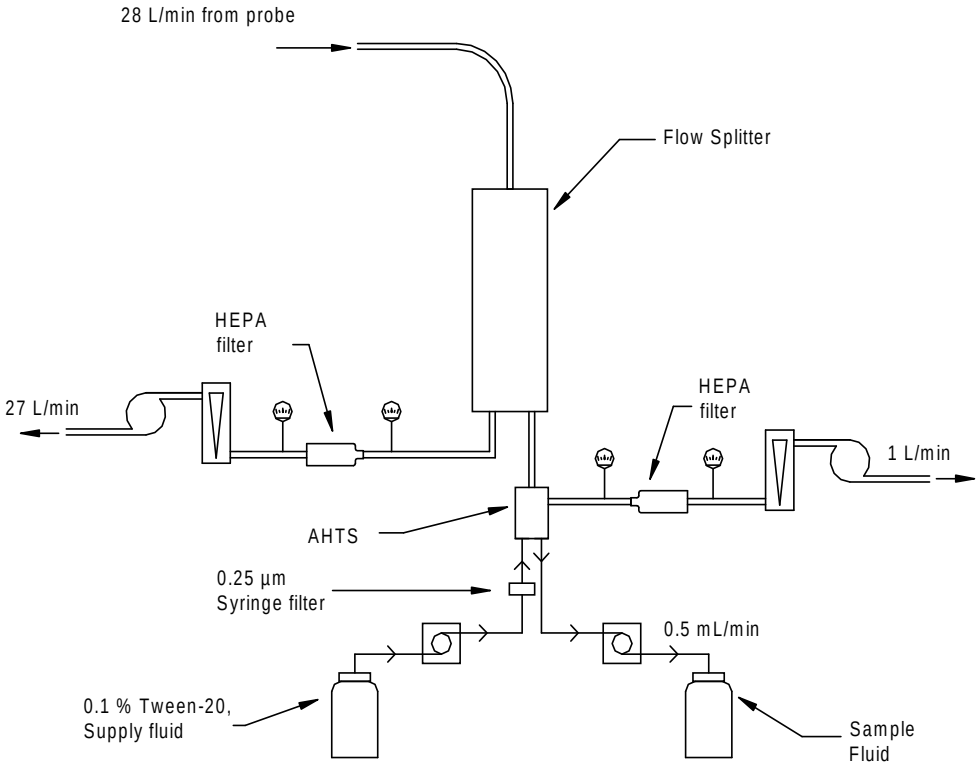

Figure 6. Setup of reference using the AHTS.

incoming air passes through the center hole to the AHTS for collection of particles with an aerodynamic diameter, D_a, greater than or equal to the 0.8 μm. Air sampled by the AHTS also passes through a similar HEPA filter before it is exhausted. Filtration of the exhausted flows is required to avoid potential contamination of the experimental setup.

Pressure is monitored upstream and downstream of the filters and the flow rate is monitored using a 0-40 L/min rotameter (Dwyer Instruments Inc., Michigan City, IN). Flow rates through the rotameters were corrected for deviations from atmospheric pressure using:

$$Q_{stp} = Q_R \sqrt{\frac{\rho_{in}}{\rho_{stp}}} \qquad [3]$$

where Q_R is the flow rate read off of the rotameter, ρ_{stp} is the density of air at standard conditions, Q_{stp} is the flow rate corrected for standard conditions, and ρ_{in} is the inlet density of air (Avalone and Baumeister 1996). Using the ideal gas law, $P = \rho RT$, the inlet pressure, measured using Minihelic II pressure gauges (Dwyer Instruments Inc., Michigan City, IN), and the atmospheric pressure may be substituted for their respective densities (Wark 1988).

Reference Setup for Collection using Filters

The reference system shown in Figure 7 was used to determine the mass emission rate and the size distribution of both the background aerosol and a bioaerosol emitted from an envelope. In this system, air is sampled using both probes concurrently. One flow is processed to remove particles of a certain size from the airstream whereas the other is not. This setup allows for the comparison of collection of mass with a size less than a particular D_a with that of the total amount of particulate mass that could be collected.

The device used to trim large incoming particles is a cyclone that was designed using the dimensions for a Stairmand high efficiency cyclone (Cooper and Alley 1994). The cyclone is designed for a flow rate of 28.3 L/min with a D_{50} of 10 μm. The design for the cyclone deviated from Stairmand design in order to accommodate an inlet and outlet

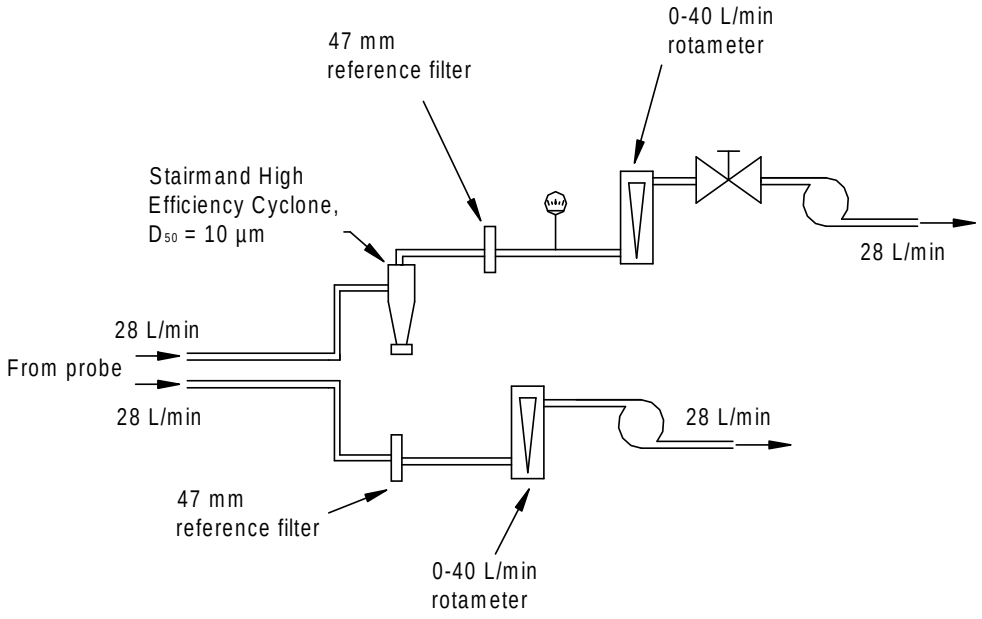

Figure 7. Reference system used for the collection of both the total material and the material of a size less than D_{50}.

with similar dimensions (25.4 mm). The deviation was based on relations proposed by Moore and McFarland (1993). According to this paper, the D_{50} of this cyclone may be calculated using:

$$ln\,(D_{50}/D_c) = ln\,a + b\,ln\,Re_f \qquad [4]$$

D_c is the cyclone body diameter, a and b are constants, and Re_f is the Reynolds flow number. The Reynolds flow number may be calculated using:

$$Re_f = \frac{\rho\,(D_c - D_o)\,U_i}{2\,\mu} \qquad [5]$$

For Re_f, ρ and μ are the density and viscosity of air respectively, D_c is the cyclone body diameter, D_o is the cyclone outlet diameter, and U_i is the inlet velocity (Q_s/A_i).

Sampling Devices

Downstream of the probes, the duct expands to a box that is 203 mm to a side. Here the flow is turned 90° and passes through a single jet impactor. Previous in-lab tests have shown that the impactor is required for two reasons: 1) to prevent clogging of delivery fluid lines and 2) to prevent clogging of a filter associated with one detection scheme. Additionally, high mass loading of the sample fluid may result in interference with the device signal associated with the bacteria. The impactor replaces a PM-10 cyclone that was previously used as the trimming device. As its name suggests, this cyclone was designed for a D_{50} of 10 μm. Midway through the study, the cyclone was removed in an attempt to capture all particles. However, the detectors were overwhelmed by debris and the system was not able to deliver a sample at the flow rate required due to clogging of the output fluid line of both cyclones. The impactor was preferred in this study over the cyclone due to space limitations and ease of maintenance.

The design of the impactor is based on relations presented in Hinds (1999, p. 126). The impactor was designed for a D_{50} of 10 μm using the following equation:

$$D_{50} = \left(\frac{9\,\pi\,\mu\,D_j^3\,Stk_{50}}{4\,C_c\,\rho_p\,Q_s} \right)^{\frac{1}{2}} \qquad [6]$$

where the slip correction factor, C_c, can be assumed to be one (because the size particle that is trimmed from the flow is large enough so that free molecular effects are negligible), μ is the viscosity of air, Q_s is the system flow rate, D_j is the diameter of the impactor jet, and ρ_p is the density of the particle (in this case, 1000 kg/m^3). The Stk_{50} is the Stokes number of a particle which is collected with 50% efficiency. The Stokes number of a particle is calculated as:

$$Stk = \frac{\rho_p\,D_p^2\,U\,C_c}{18\,\mu\,W} \qquad [7]$$

The Stokes number is the particle stopping distance relative to a characteristic dimension in the flow, W. For an impactor, W is the jet half-width, $D_j/2$. A D_{50} of 10 μm for the trimming impactor was chosen based on collected filter and impactor data concerning

background and bioaerosol size distributions.

The diameter of the jet impactor was solved for iteratively by using Equation (6) and then evaluating the Reynolds number of the jet. The Reynolds number for the jet, Re_j, is calculated as follows:

$$Re_j = \frac{\rho\, Q_s\, D_j}{\mu\, A_j} \qquad [8]$$

where A_j is the jet cross sectional area. For the initial calculation, the $\sqrt{Stk_{50}}$ for a round jet impactor cited in Hinds (1999, p. 126) was used. Using Equation (8) with 1.2 kg/m^3 and 1.81×10^{-5} Pa·s as the density and viscosity of air respectively, the Re_j is 2.6×10^4. According to Marple and Liu (1974), the $\sqrt{Stk_{50}}$ for this value of Re_j should be ~ 0.43 for round jet impactors. Solving Equation (6) using a jet diameter of 38 mm and a $\sqrt{Stk_{50}}$ of 0.43, the D_{50} of the impactor is 10 μm.

The jet contracts from an inlet diameter of 76 to 38 mm. The jet to surface separation is approximately one jet diameter. In a study on collection characteristics of impactors, Rao and Whitby (1978) found that an impactor with an oil coated glass plate as the impaction surface had much better collection characteristics than a un-coated surface or a glass fiber filter. The reason for the differences in collection efficiencies for different surfaces is related to particle bounce and blow-off. For this reason, the impaction surface used in this study was a transpirated material soaked in diffusion pump oil. Particles with an D_a greater than 10 μm are impacted on this surface.

Downstream of the impactor, the system contracts to a diameter of 76 mm where the flow enters the collection device. In this study, two different wetted-wall cyclones were evaluated as the system collection device. The first of these was a glass cyclone sampler (GCS), also known as the Aerojet General Liquid Scrubber Sampler (Decker et al. 1969). The second device tested was the cyclone that is used in the Army's Joint Biological Point Detection System (JBPDS). Both cyclones are operated at 780 L/min and a delivery fluid flow rate of ~ 1 mL/min.

There are several advantages for using a wetted-wall cyclone versus collection on a

nutrient medium or some other surface suitable for the collection of bioaerosols. The first is that the output may be assayed in a variety of ways. At this point in time, this system requires a liquid sample to be used by the detectors for real-time analysis. Also, when collecting biological material using a "wet" medium (especially one containing a surfactant such as 0.1% Tween-20), the bioaerosol is more likely to break up into individual particles (spores) (Macher 1999). Therefore, colonies counted on plates from these samples are more likely to arise from a single spore or cell. This manner of collection also reduces particle bounce and dry deposition, therefore sharpening the efficiency curve of the device and increasing the amount of recoverable material (Rao and Whitby 1978). Finally, the collection of material using wetted wall was reported by Griffiths et al. (1997) to result in greater viability of biological particles than collection on a dry medium.

The flow rate of the collection system is monitored using a venturi meter (Lambda-Square, Babylon, NY). A control loop for the system blower using the differential pressure output of the venturi meter as the input was developed by Siemens Dematic. The flow rate for this system is 780 L/min. This flow rate is based on an optimal aspiration efficiency of the system and the D_{50} of the cyclones. To maintain a constant flow rate through the venturi meter, the differential pressure must be adjusted for the inlet fluid density. Curves for the differential pressure versus the flow rate at different inlet fluid densities are shown in Appendix B.

Glass Cyclone Sampler

The first cyclone used in this study was the Glass Cyclone Sampler (GCS). In this cyclone, a nebulized solution of 0.1% Tween-20 is introduced into the flow immediately upstream of the cyclone inlet. The nebulizer consists of two needles with an inner diameter of 0.6 to 0.8 mm (18 to 20 gauge) meeting at a confluence. High pressure air, 102 to 206 kPa (gauge pressure), flows through the needle parallel to the airflow in the duct immediately upstream of the cyclone. A 0.1% Tween-20 solution flows through another

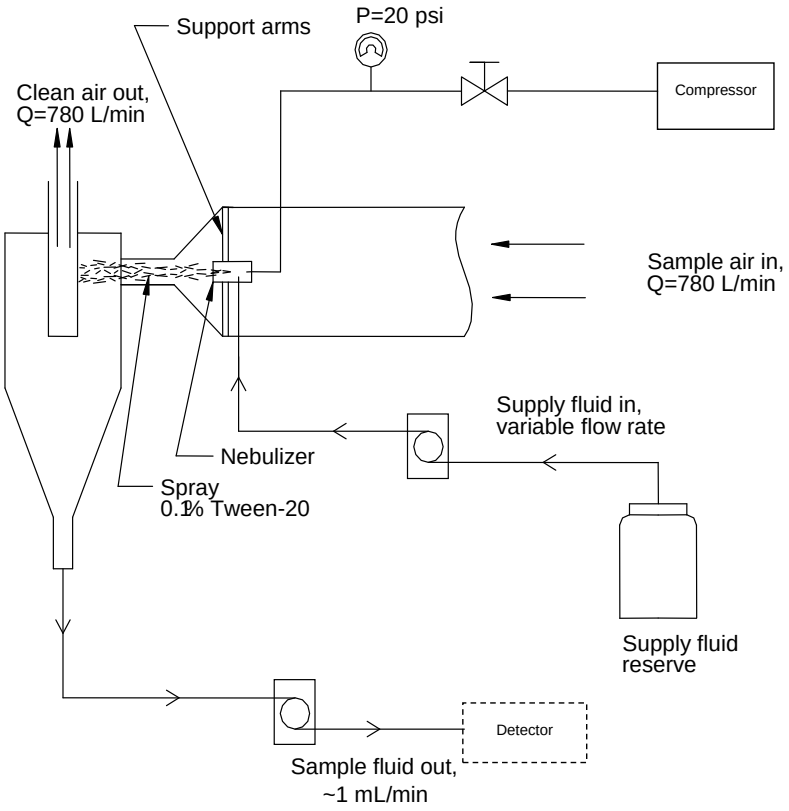

Figure 8. Schematic showing the introduction of the nebulized spray to the glass cyclone.

needle perpendicular to the airflow. Flow of that solution is controlled using a peristaltic pump (Cole Parmer Instrument Co., Vernon Hills, IL). As it flows through this latter needle, the solution is atomized by the high pressure air. This atomized solution is a fine mist that coats the initial impaction zone. The nebulizer takes up a minimal amount of the cross sectional area in the incoming duct. A schematic of the cyclone in relation to the nebulizer and the incoming air is shown in Figure 8.

Shear forces of the airflow drive the solution about the wall of the cyclone thereby allowing particles to be captured and drawn-off in a liquid suspension from the bottom. The output fluid is extracted at a rate of approximately one mL/min. The output fluid is either collected in a conical tube for laboratory analysis, or, in the case of integrated operation, connected to a detector for real-time analysis.

Table 1. Estimated cutpoint of the Aerojet glass based on empirical models and experiments. (a) Moore and McFarland (1993), (b) Iozia and Leith (1989), (c) Upton et al. (1994), experimental result.

Q	D_{50} (μm)		
(L/min)	(a)	(b)	(c)
500	0.99	1.21	1.5
567	0.9	1.14	
710	0.75	1.02	
780	0.69	0.97	
852	0.65	0.93	
993	0.57	0.86	

As a bioaerosol sampler, the GCS has been studied extensively. In a study by Upton et al. (1994), the D_{50} (based on collection efficiency) of the GCS was experimentally found to be 1.5 μm at 500 L/min. In another study, Griffiths and Boysan (1996) developed a CFD model, validated using Upton et al.'s (1994) data, for the GCS. In this study, they compared their results to the experimental data and several other models. They found that no model was exceptionally suitable for this cyclone, but that the model postulated by Iozia and Leith (1989) was able to correctly calculate the D_{50}.

Although the model of Moore and McFarland (1993) was developed for the Stairmand cyclone, the calculation of D_{50} for the GCS is shown in Table 1 along with the calculation of D_{50} using Iozia and Leith's model. The dimensions for the GCS are given in Griffiths and Boysan's study. Both Moore and McFarland's and Iozia and Leith's models appear to under-predict the D_{50} of the GCS (compared to Upton et al.'s experimental data); however, Iozia and Leith's is closer to the actual D_{50} at 500 L/min than Moore and McFarland's. A theoretical fractional efficiency curve for the GCS operating at 780 L/min is shown in Figure 9. This curve is based on a logistic function proposed by Iozia and Leith (1990). This curve was calculated using the function:

$$\eta_c = \frac{1}{1 + (D_{50}/D_p)^{\beta}} \qquad [9]$$

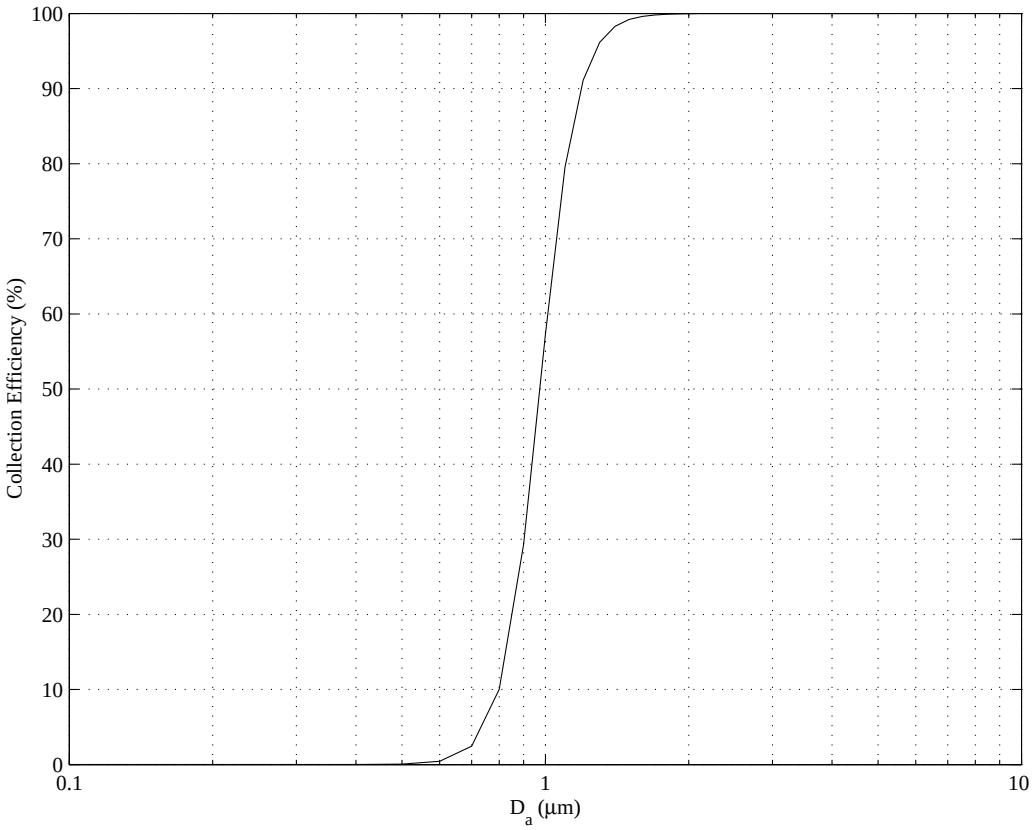

Figure 9. Fractional efficiency curve for the GCS operating at 780 L/min. Curve is based on the logistic function proposed by Iozia and Leith (1990).

where D_p is particle diameter and β is the logistic slope parameter calculated using functions given in Iozia and Leith (1990). However, it was previously noted that although the D_{50} appears to be correctly predicted (compared with experimental data), the curve itself is too sharp (Griffiths and Boysan 1996).

The JBPDS Cyclone

The other wetted-wall cyclone that was tested with this system is the cyclone that is used in the Joint Biological Point Detection System (JBPDS) for the Army and was developed at Battelle (Black 2002). This cyclone is designed to be operated with its axis parallel to the ground. Similar to other cyclones, air enters this device tangentially and particles larger than the D_{50} of this device impact against the wall due to the centrifugal

force exerted on the particles as the flow is turned. The walls of the cyclone are wetted by a solution of 0.1% Tween-20 that flows at $\sim$ 1 mL/min through an array of small holes in the inlet of the device. The liquid is spread across the surface of the cyclone by the shear forces generated by the incoming air. Contrary to traditional cyclones, the air flow is not turned at the bottom so that it may exhaust through the top. Instead, the sampled air exits through the bottom of the cyclone. The D_{50} of this cyclone at 780 L/min is approximately 0.8 μm (Black 2002). In tests at Battelle, the biological sampling efficiency for a population of BG spores with a mass-median aerodynamic diameter of 1.9 μm was 61%.

EXPERIMENTAL PROCEDURE AND ANALYSIS

To characterize the system, tests were run to quantify the release of bacteria from an envelope as well as various aspects of background emissions from the mail sorting process. In the former case, the release of the bacteria was quantified in terms of the released size distribution, the amount that was greater than a D_a of 10 μm, and the amount collected by the three different devices. For the latter case, emission rates, the size distribution of the emission, and the mass of particles captured with a D_a less than 10 μm were quantified relative to the mass of all particles captured. Prior to the above characterizations, tests were performed at various flow rates to determine the aspiration efficiency of the system. Finally, the system response time was characterized relative to a bioaerosol release for both the JBPDS cyclone and the GCS.

Aspiration Efficiency

Aspiration efficiency tests were conducted to ensure that the system could sample an optimum amount of the material that might be released by the mail sorting process. These tests were conducted for four flow rates ranging from 560 L/min to 990 L/min. In each test, a tracer gas was released at two points along the perforated plates, immediately upstream of the hood. These release points simulated a release of particles from the bottom and the top of an envelope. Tests were conducted while mail was moving and while mail was not moving.

The tracer gas chosen consisted of 1000 ppm sulfur hexafluoride, SF_6 (Specialty Chemical Products, Inc., South Houston, TX). Using a syringe pump, the gas was released at a rate of 21 mL/min. A sample was extracted immediately upstream of the reference probes. Samples were extracted 60 mL at a time using a syringe attached to tubing. The tubing protruded into the center of the duct.

The aspiration efficiency, η_a, is the ratio of the gas collected versus the gas released

and can be calculated using:

$$\eta_a = \frac{C_{s,SF_6}}{C_{i,SF_6}} \quad [10]$$

where,

$$C_{i,SF_6} = 0.1\% \times \frac{Q_{SF_6}}{Q_{SF_6} + Q_s} \quad [11]$$

and Q_{SF_6} is 21 mL/min and Q_s is the system flow rate (560 to 990 LPM). The system concentration, C_s, was evaluated by analyzing the 60 mL samples collected using an Autotrac gas chromatograph (Lagus Applied Technology, Inc., San Diego, CA).

Characterizing Background Emissions

Background Emission Rate and the Relative Mass

The first set of tests conducted with the intent of characterizing background emissions was the quantification of aerosol emission rates. These were conducted in two ways. The first set of tests was to determine the emission rate as a function of system flow rate. The second set of tests were used to determine the mass fraction of material emitted that had a D_a less than 10 μm.

For both sets of tests, the reference system shown in Figure 7 was used. In the first set of tests, only one probe was utilized. A sample was extracted through the probe to which a filter holder containing a 47 millimeter, Type A/E glass fiber filter (Pall Gelman Sciences, Ann Arbor, MI) was attached. The sample was extracted at a rate of 28.3 L/min. Standard gravimetric techniques (Willeke and Baron 1993) were used to measure pre- and post-sample filter mass. These measurements were taken using a Mettler H51AR Analytic Balance (Mettler-Toledo, Princeton, NJ) which has a sensitivity of $\pm$0.01 mg. The mass emission rate, in mg/min, was calculated as:

$$\dot{m} = \frac{\Delta m_f}{t_s} \frac{Q_s}{Q_p} \quad [12]$$

where Δm_f is the change in the filter mass after collection, Q_p is the probe flow rate (28.3

L/min) , and t_s is the total sampling time. Each sample was weighed several times and the mean of the mass measured is reported for Δm_f. Samples were charged neutralized before weighing and weighed repeatedly over several days to verify that there was no significant weight gain or loss due to changes in relative humidity in the facility. Samples taken to determine the mass fraction of material with a D_a less than 10 μm were conducted in a similar manner. However, for these tests, both probes were used, the second one being attached to the trimming cyclone. A filter was placed immediately downstream of the cyclone.

Size Distribution of the Background Aerosol

In the characterization of the background, the size distribution of material from the mail sorting process was measured in two ways. The first way was to measure the size distribution of the effluent aerosol. In this case, a sample was extracted from the main flow using a reference probe (without a trimming cyclone) as stated in the previous section. Material was collected on a 47 millimeter, Type ATTP Membrane filter (Millipore, Bedford, MA) with a pore size of 0.8 μm. After a sample was taken, the filter was transferred to a beaker containing a 10 mL solution of 0.1% Tween-20. The beaker was then placed in an ultrasonic bath for one minute in order to remove particles from the filter. The filter was removed from the solution and a sample was pipetted from the resulting solution. This pipetted sample was then placed in an Accuevette containing Isoton-II, an electrolytic solution used by a Multisizer 3 Coulter Counter (Beckman-Coulter, Brea, CA). This solution was then analyzed using the Coulter Counter, which develops particle statistics for a sample solution relative to a volume equivalent diameter, D_e. The relationship between D_e and the aerodynamic diameter, D_a, is:

$$D_a = D_e \sqrt{\frac{\rho_p}{\rho_o \chi}} \qquad [13]$$

where ρ_o is unit density (1000 kg/m^3) and χ is the particle shape factor (Hinds 1999, p. 54).

The relationship between a particles volume equivalent diameter and its aerodynamic equivalent diameter is complex. This issue is illustrated by Figure 10. This figure shows a membrane filter used to capture unprocessed background emissions. On the filter surface are several long fibers. Although it is not difficult to find D_e, it is not possible to accurately calculate a size distribution generated using the Coulter Counter and extrapolate for a size distribution based upon D_a. This is because the aspect ratio, which is a factor that affects χ, of these fibers generated by the mail sorting process is not necessarily uniform. However, the size distribution of background emissions is relevant because the volume of material generated will possibly affect the signal in a detector generated by any BG.

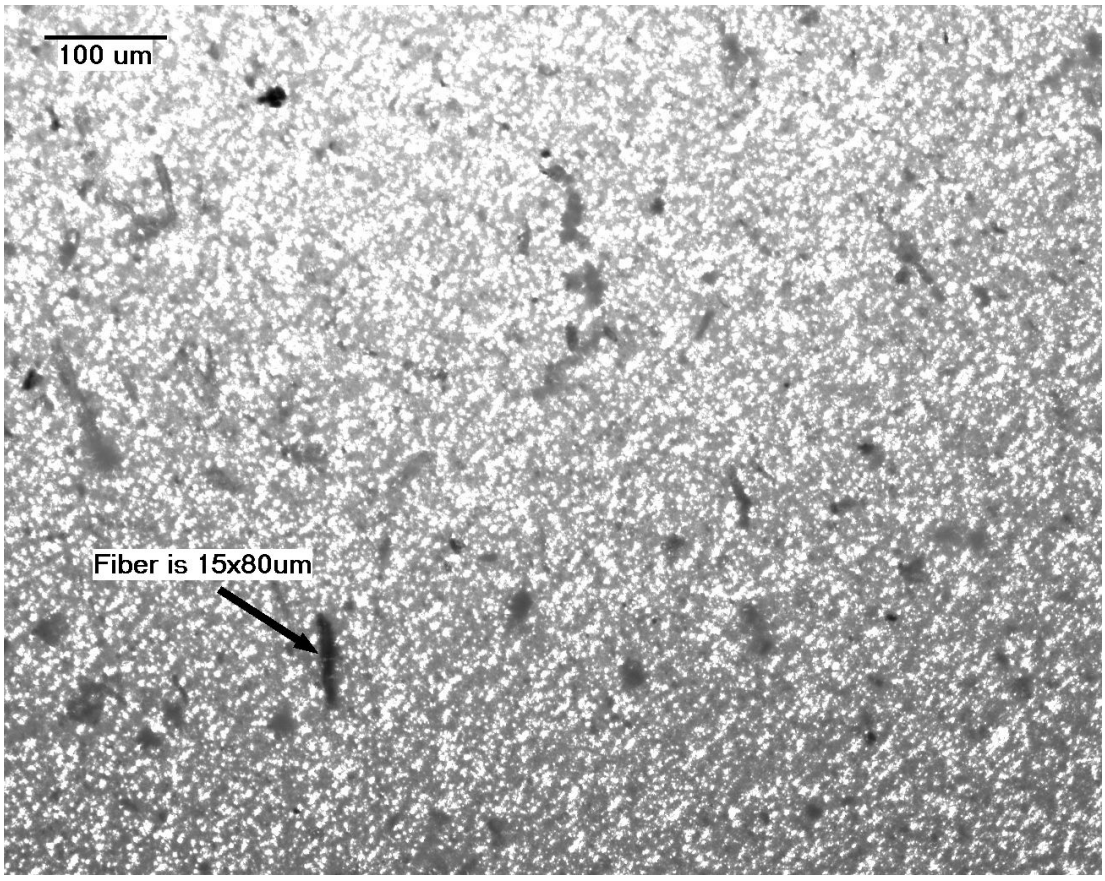

Figure 10. Microscopic image of filter used to capture background emissions.

The other size distribution measurement taken was that of each device output fluid. The analysis for these samples was performed using the Coulter Counter in a manner similar to the analysis done on the filters (as outlined above). However, with the output sample fluid from each device, no intermediate processing was required to prepare the sample for analysis using the Coulter Counter. In this case, an appropriate amount of sample fluid was pipetted into a volume of Isoton II. The resulting solution was placed in the Coulter Counter and analyzed as above.

Characterization of a Bioaerosol Release

In the current context, the bioaerosol particles of interest are *Bacillus anthracis* (also known as anthrax) spores. Anthrax is a gram-positive, endospore forming, zoonotic pathogen (Prescott et al. 1996). The vegetative cell is rod shaped, whereas the spore is oval. In a US army study using cynomolgous monkeys, the LD_{50} (a lethal dose for 50% of subjects) was reported by Peters and Hartley (2002) to be 8000 spores. There are currently no reliable numbers concerning the LD_{50} of anthrax in humans. However, the LD_{50} for a human may be significantly lower depending on the health of that individual.

For biological testing, *Bacillus globigii*, or BG, was used as a simulant for anthrax. BG has aerodynamic properties similar to *B. anthracis* and is not pathogenic. Anthrax spores appear to have a D_a between 1 and 3 μm. This number is based on a study by Weis et al. (2002) in which air samples were taken in an office contaminated with anthrax under simulated active conditions. In these studies, Anderson viable 6-stage impactors were used and the majority of spores captured were present on the last two stages ($D_a < 2.1$ μm) with a small but significant number being captured by the third stage ($D_a < 3.1$ μm). According to Quian et al. (1997), the aerodynamic diameter of BG is 0.8 μm. The simulant, BG, was provided by the Army Research Laboratory (ARL) from the Dugway Proving Grounds in Utah in the spring of 2002. The spore preparation was maintained at temperature of 8°C. Consistent with those numbers cited by Kournikakis

et al. (2001), who also received BG from Dugway, the spore preparation was found to have a concentration of 3×10^{11} CFUs/g. This was verified by plating sample suspensions of the spore powder.

Four types of biological testing were performed: one to determine the size distribution of material released, one to determine the amount of material and classify by size the bioaerosol that might be released, another to determine the amount of material that might be captured by a device given a release, and a final test to determine the response time of the system. In order to simulate a biological release, envelopes were loaded with a known amount of BG using the same techniques as those applied by Kournikakis et al. (2001). The BG was placed in a tri-folded piece of paper and that piece of paper was then placed in a self-sealing envelope. Care was taken to ensure that the BG remained in the piece of paper while loading the envelope. The envelope was then placed in the incoming mail stack upstream of the joggers and allowed to pass once through the feeder. All reference pumps required for collection were activated approximately 10 seconds prior to the release. Whenever possible, several different types of tests were run concurrently.

Determining the Size Distribution

Although the aerodynamic diameter of a single BG spore is approximately 0.8 μm, the microbiological material emitted from an envelope may considerably larger than this. This is because the bacteria may be distributed in the envelope in clumps and not dispersed as it is released from the envelope. An example of a clump of spores is shown in Figure 11. Because the system must be designed to capture the greatest number of spores from a release, it is necessary to know the size distribution of the material released, particularly in relation to the volume of the clumps. The greater the volume of the clump (i.e. the larger the aerodynamic diameter), the greater the number of spores (assuming a homogeneous clump).

An Anderson 6-stage viable cascade impactor (Thermo-Anderson, Smyrna, GA) was

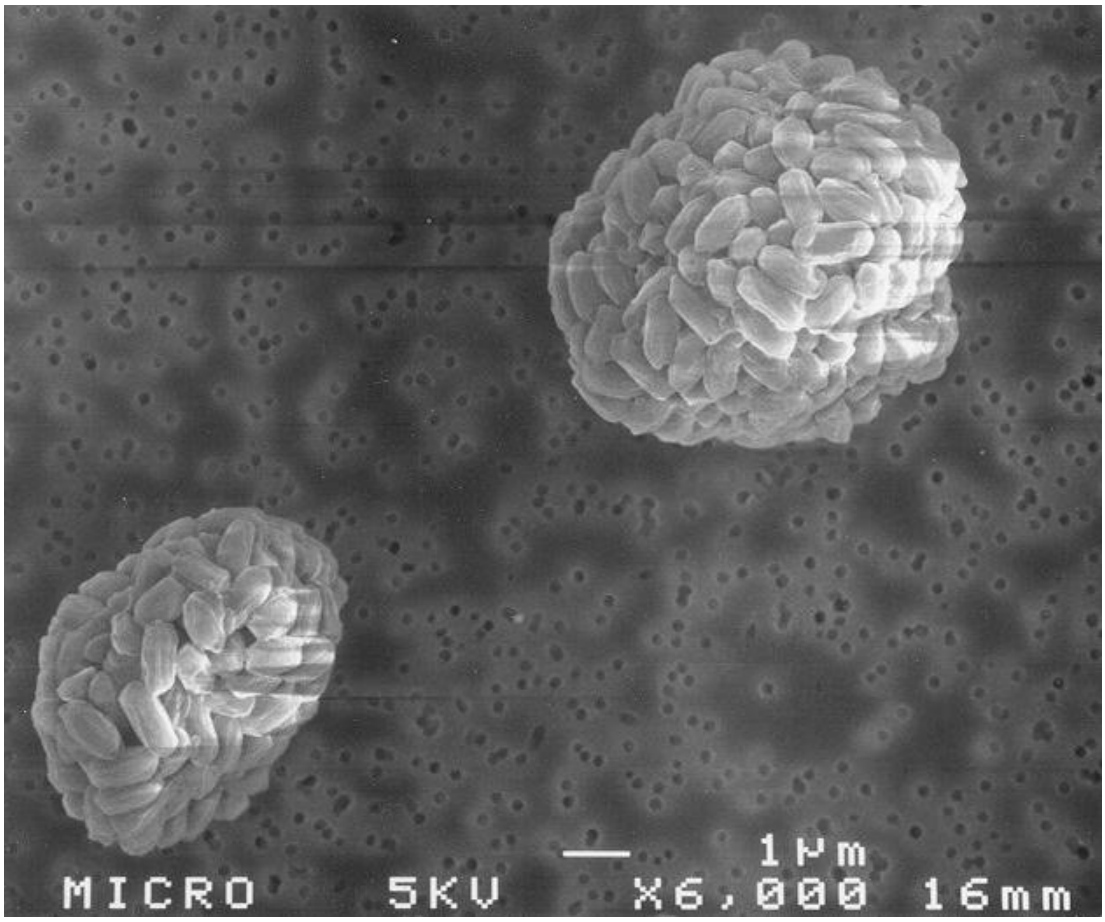

Figure 11. SEM image of two clumps of BG spores.

used to determine the size distribution of the biological material released from an envelope during a simulated bioaerosol event. Each of the six stages of the impactor consist of 400 jets, distributed symmetrically in a circular pattern. These jets accelerate the flow through the device, causing particles larger than the cutoff size of that stage to impact on a surface containing a suitable growth medium. In the case of these tests, the impaction surface consisted of a plate of tryptic soy agar (TSA) prepared by PathCon (PathCon Analytical Products, Nocross, GA). The plate contained an amount of agar that maintains the proper jet-to-surface height as outlined in Anderson (1958). The cutpoint of each stage is given in Table 2. Also shown in Table 2 is the potential number of spores present in a colony of *B. subtilis* on a stage, as postulated by Anderson (1958). For this study, stage one refers to the topmost stage.

Table 2. The lower bound D_a for each stage of the Anderson impactor. Column three gives the estimated number of BG cells per particle captured on a stage as reported by Anderson (1958).

Stage	D_{50} (μm)	Estimated spores per particle
1	7.2	150 to 1000+
2	4.8	22 to 200
3	3.2	9 to 25
4	2.1	3 to 10
5	1.0	1 to 4
6	0.6	1

The reference setup in Figure 7 was used to extract a sample through the impactor for one minute as an envelope was run through the machine. In these tests, one probe was used without a trimming device. The pump controlling the flow through the impactor was powered on approximately 10-15 seconds prior to the release and the impactor was operated for approximately 1 minute after the release. The plates were then removed from the impactor and the samples were stored and incubated as stated in the following section on microbiological analysis. The colonies were counted using a Bantex 920A Colony Counter (American Bantex Corp., Burlingame, CA) and a positive-hole correlation (PHC) was used to account for multiple colonies at one site.

The PHC describes the probability that if x amount of impaction sites are filled (a "positive hole"), then y amount of particles may be found at one of those sites. The positive hole conversion formula is:

$$N_p = N_j \times \sum_{x=0}^{n+1} \left(\frac{1}{N - x} \right) \qquad [14]$$

where N_p is the estimated number of viable particles present, N_j is the total number of jets per stage (400), and n is the number of filled holes. This correlation was validated in a Monte-Carlo study by Macher (1989). According to the study by Macher, when 200 holes are filled (positive), the coefficient of variation (COV) for the expected number of

colonies is 4%. From this same study, the COV for 400 positive holes (a colony associated with each jet) is 19.4%. According to both Macher and Anderson, the PHC may not be used for the top two plates. The reason for this is that particles will not impact immediately below the jet, thereby making it difficult to determine whether more than one visible colony came from a single jet. On the top two plates, all colonies are counted as if they arise from individual cells. On subsequent plates, where the PHC is applicable, coincidental colonies and colonies present outside of the jet pattern are not counted.

Capturing Bacteria Using a Filter

In another set of experiments (run concurrently with device capture tests), gelatin filters were used to characterize the amount of bacteria released during a bioaerosol event. These filters were used to characterize both the total amount released and the amount with a D_a less than 10 μm. For these experiments, Sartorius gelatin filters (Sartorius, Goettingen, Germany) were used.

Filters were placed inline with the two reference probes. Similarly to the characterization of the background mass emission rates, one filter was placed downstream of a Stairmand high efficiency cyclone with a D_{50} of 10 μm, while the other filter sampled unprocessed air. In both cases, the sample pumps were activated approximately 15 seconds before the release and operated for approximately 1 minute after the release.

Upon completion of the test, these filters were transferred to sterile, 50 mm petridishes (Pall Gelman Sciences, Ann Arbor, MI) and stored at 8°C. There were two possible methods that could be used to culture these samples: the direct method in which a filter is placed directly on a growth medium, and the indirect method. The indirect method involves the dissolution of the filter in a warm, sterile medium. In this method, large clumps of bacteria are broken up and colonies counted using this method are more likely to arise from single cells. For these experiments, the indirect method was used for the analysis. Since the indirect method was used to culture the bacteria, there was no growth

medium within the dishes used to store the filters.

Device Output and the System Response Time

For each device with a liquid output (the AHTS, GCS, and the JBPDS cyclone), a set of experiments was run to characterize the device collection in terms of colony forming units (CFUs) as a function of the mass of BG in an envelope (in mg). Tests were run as outlined previously in this chapter. Collection of the output fluid began immediately after the release event. The output fluid was collected in a 15 mL, conical tube (Becton Dickinson Labware, Franklin Lakes, NJ). Based on previous in-lab tests, the total collection time for each device was set to 5 minutes. For the characterization of the system response time, samples were collected at 30 or 60 second intervals (60 seconds for the GCS and 30 seconds for the JBPDS cyclone). In each experiment, the output fluid was diluted as necessary and an appropriate amount of fluid was cultured (as described in the following section).

Microbiological Analysis

Samples containing BG were analyzed using standard microbiological techniques (Cruickshank 1960). The microbiological analysis performed in this study is based on the culturability of the material captured. Although the term "viability" is used interchangeably with culturability, in both cases the intended meaning is the ability of a material to grow on a particular medium (Griffiths et al. 1996; Henningson et al. 1997). However, a study by Griffiths et al. (1996) showed that for hardy organisms such as spores, the culturable fraction should remain constant. In the case of the experiments performed here, the medium used for culturing samples was tryptic soy agar (TSA) (Becton, Dickinson, and Co., Sparks, MD).

As stated in the previous section, sample filters were processed for bacterial counts using the indirect method. In this case, the filters were dissolved in a sterile solution of

0.1% Tween-20 maintained at 37°C. For dissolution, the 10 mL of the sterile solution was placed in a 150 mL beaker. The filter was then carefully added to the solution so as to avoid contact with the sides of the beaker. After the filter was placed in the solution, a sterile, teflon coated magnetic stirring bead (Fisher Scientific, Pittsburg, PA) was added and the suspension was stirred using a magnetic stirrer (Barnstead|Thermolyne, Dubuque, IA) for 30 seconds or until the filter appeared to be completely dissolved. After the filter was dissolved, the suspension was transferred to a 15 mL conical tube for storage. The solution was later diluted as necessary and then plated. In the case of the samples extracted using the Anderson impactor, there was no additional sample preparation required for culturing.

With all liquid samples, serial dilutions were performed as necessary such that the final CFU count on a plate was between 25 and 400. Optimally, the total count should be between 100 to 250; this number provides statistically better results while avoiding potential overcrowding problems associated with numbers greater than 250 CFUs (Cruickshank 1960). Before dilutions were performed or final samples were plated, each tube was vortexed for 30 seconds using a Fisher Touch Mixer, Model 231 (Fisher Scientific, Pittsburg, PA). To ensure statistical significance, samples were plated using a 25-250 μL pipettor (Brinkmann Instruments, Westbury, NY) three times. In most cases, the amount plated was 100 μL, but the final amount plated was based upon the concentration of bacteria within the suspension.

All cultured samples (including those taken from the Anderson impactor) were placed in an incubator set to 37 °C for a period of 12 to 13 hours, as specified in *Bergey's Manual* (Breed et al. 1957). This period of time allows BG colonies to grow to a size at which the they may be identified and counted, but not to the point where there is dramatic colony overlap. The colonies were identified using the information provided in *Bergey's Manual* and counted. Because the environment in which the mail sorting machine operates is not sterile, background contamination was inevitable. Throughout all tests, background levels of BG were monitored. For the device tests, the amount of BG

released was increased in increments. A space of at least fifteen was allowed between test runs. This prevented significant overlap between tests. It was shown in previous studies that secondary aerosolization from surfaces is insignificant relative to the primary event (Centers for Disease Control and Prevention 2001a; Weis et al. 2002). Since the majority of overlap in the device appeared to be due to residence within the tubing and device itself, it was not necessary to run tests in an increasing manner while collecting on only a filter medium.

In the chapter detailing results, all fluid and filter samples are plotted as total CFUs collected versus the amount of bacteria in the envelope. The number of CFUs collected was calculated using:

$$N = \bar{n}\, DF\, \frac{V_o}{V_p} \qquad [15]$$

In this case, $\bar{n}$ is the average number of CFUs counted for all plates from the sample, DF is the dilution factor, V_o is the total volume collected (in mL), and V_p is the volume plated (mL). The dilution factor, DF, is non-dimensional and has the value of a positive integer such as 10, where a 1:10 dilution was performed.

RESULTS AND DISCUSSION

In the following sections, the results of the experiments run to characterize the system are presented. The tests characterized the aspiration efficiency of the system, the background emissions, and the release of bioaerosols. In general, each type of test was run multiple times; therefore, the results given are the mean of the tests run, unless otherwise specified. Much of the data used to generate the following plots are given in the appendices.

Before the system could be characterized with respect to background and bioaerosol emissions, it was necessary to verify that the system could collect a significant amount of the emissions. In order to do this, tests were run to determine the aspiration efficiency of the system. The results are given in Figure 12. The plot in Figure 12(a) shows the aspiration efficiency of the system with the mail moving. This is contrasted with Figure 12(b), which shows the aspiration efficiency of the system without mail moving. The results for an upper and lower release are plotted for both scenarios. The error bars shown in each plot are based on the standard deviation of multiple measurements (uncertainty

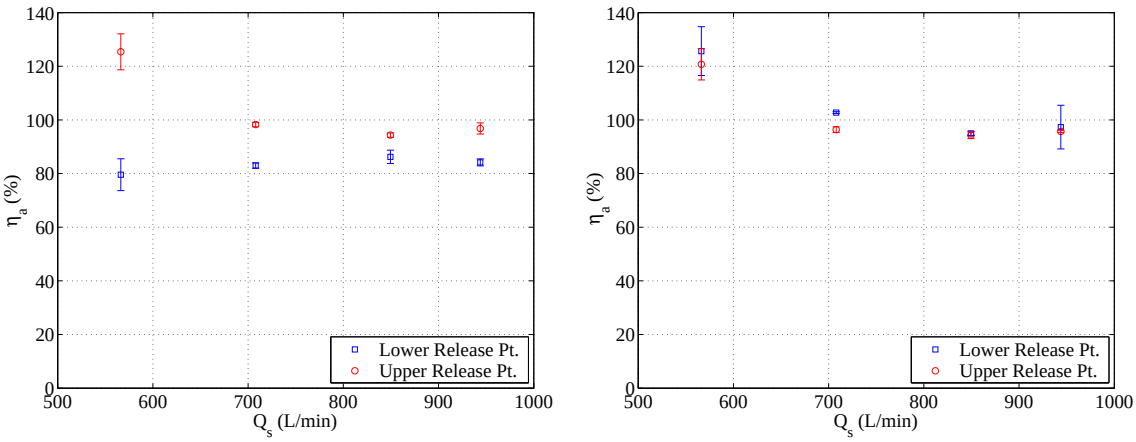

Figure 12. Aspiration efficiency, η_a, for two release points with (a) mail moving and (b) with no mail moving.

due to repeatability).

As can be seen from these plots, the aspiration efficiency for the upper release is close to 100% for both scenarios. However, in both cases, the upper release for lower flow rates is significantly greater than 100%. This is also the scenario for the lower release with no mail moving. This may be caused by poor mixing at these lower flow rates. At a flow rate of 550 L/min, the Reynolds number, calculated using Equations (1) and (8), is 5.8×10^3. At 780 L/min, the Reynolds number at the sampling point is 8.2×10^3. McFarland et al. (1999) showed that the mixing in a duct improved as the Reynolds number increased. Although the difference in Reynolds numbers appears to be small, this may affect the mixing enough to give the results shown in Figure 12.

Background Characterization Results

Mass Emission Rates

As previously stated, the background was characterized in several different ways. In the first set of tests, background emissions were captured on filters with the reference system shown in Figure 7. Tests were conducted to compare the mass emission rate for three different flow rates and the mass fraction with D_a less than 10 μm at a single flow rate (780 L/min). The mass emission rate was calculated using Equation (12). It was expected that the mass emission rate would be dependent upon the condition of the mail, but independent of the system flow rate for higher flow rates. The reason the emission rates were not expected to change with the flow rate was that the aspiration efficiency, as shown in Figure 12, does not change significantly with flow rate. Data concerning mass emission rates are given in Tables 3 and 4.

The background emission rate was examined for three separate flow rates. The results are shown in Table 3. The background mass emission rate, $\dot{m}$, for each flow rate in the table is the average of the number of tests in column two. One sample was taken for each test. Throughout this set of tests, the same batch of mail was used. In these tests, the

Table 3. Total mass emission rate, $\dot{m}$, for three different flow rates.

Q_s (L/min)	Number of Tests	$\dot{m}$ (mg/min)	COV
710	7	3.12	14.5%
852	5	2.69	15.9%
993	6	3.15	10%

sample flow was not processed by a cyclone.

Using the statistical toolbox in MATLAB (The MathWorks Inc., Natick, MA), a one-way analysis of variance (ANOVA) was performed on the mass emission rate data in Table 3 in order to determine whether there was a correlation between the emission rate and the system flow rate. Before the ANOVA was performed, a Lilliefors test was run on the data to verify that the samples followed a normal distribution. In this case, each set of samples turned out to follow a normal distribution (based on a significance level of 0.05). For the ANOVA, the significance level, α, was 0.01. The result of the test was $p = 0.24$, providing insufficient evidence to reject the null hypothesis that mass emission rate does not vary with flow rate above 700 L/min. As previously stated, this result was expected. The reason for this is that at flow rates higher than 700 L/min, the aspiration efficiency is near 100%.

Table 4. Mass emission rates and the percentage that is < 10 μm.

Test	$\dot{m}_{d<10}$ (mg/min)	$\dot{m}_{tot}$ (mg/min)	% < 10 μm
1	1.91	3.21	59.40
2	1.68	2.73	61.45
3	1.87	2.72	68.92
4	2.25	3.42	65.59
5	2.51	3.81	65.84
6	2.71	3.76	72.11
Average			65.55
COV			7.13%

The test results shown in Table 4 compare the mass emission of particulate matter with size less than 10 μm (PM-10) with the total mass emission rate for a single system flow rate of 780 L/min. In each test, background was collected for a period of 15 to 20 minutes. The test time was adjusted to avoid filter overloading. All of the tests in Table 4 were run with the same batch of mail.

The mean of all tests results in Tables 3 and 4 measuring the mass emission rate for total particulate matter (PM) is 3.15±0.21 mg/min. In this context, the mean is relevant because the mass emission rate was shown not to vary significantly with flow rate. The bounds given are determined by the 95% confidence interval for the measurements. The 95% confidence interval was solved for using:

$$\bar{x} - t(1-\alpha)\frac{s}{\sqrt{n}} < \mu_s \leq \bar{x} + t(1-\alpha)\frac{s}{\sqrt{n}} \qquad [16]$$

where $\bar{x}$ is the mean of all tests evaluating the total emission rate (in mg/min), s is the standard deviation of the samples, n is the number of tests run, and $t(1-\alpha)$ is is the value from the Student's t distribution for $n-1$ degrees of freedom and a confidence interval of $1-\alpha$ (Mandel 1964). In this case, μ_s is the expected average mass emission rate which falls in the 95% confidence interval for 23 degrees of freedom.

Background Size Distribution

Once a system flow rate was established, tests were conducted to determine the background size distribution. Tests were run using the AHTS, JBPDS cyclone, GCS, and filters. Results for the JBPDS cyclone and the GCS are shown in Figure 13. For this set of tests, a 50 μm aperture tube was used with the Coulter Counter. This aperture tube was chosen based on tests conducted with several other aperture tubes. The maximum detectable size range of material with a particular aperture is 2 to 60% of the aperture. In this case, the size range was 1 to 30 μm. If the appropriate size aperture is chosen, there should be flat tails at the end of the cumulative distribution (as shown in Figure

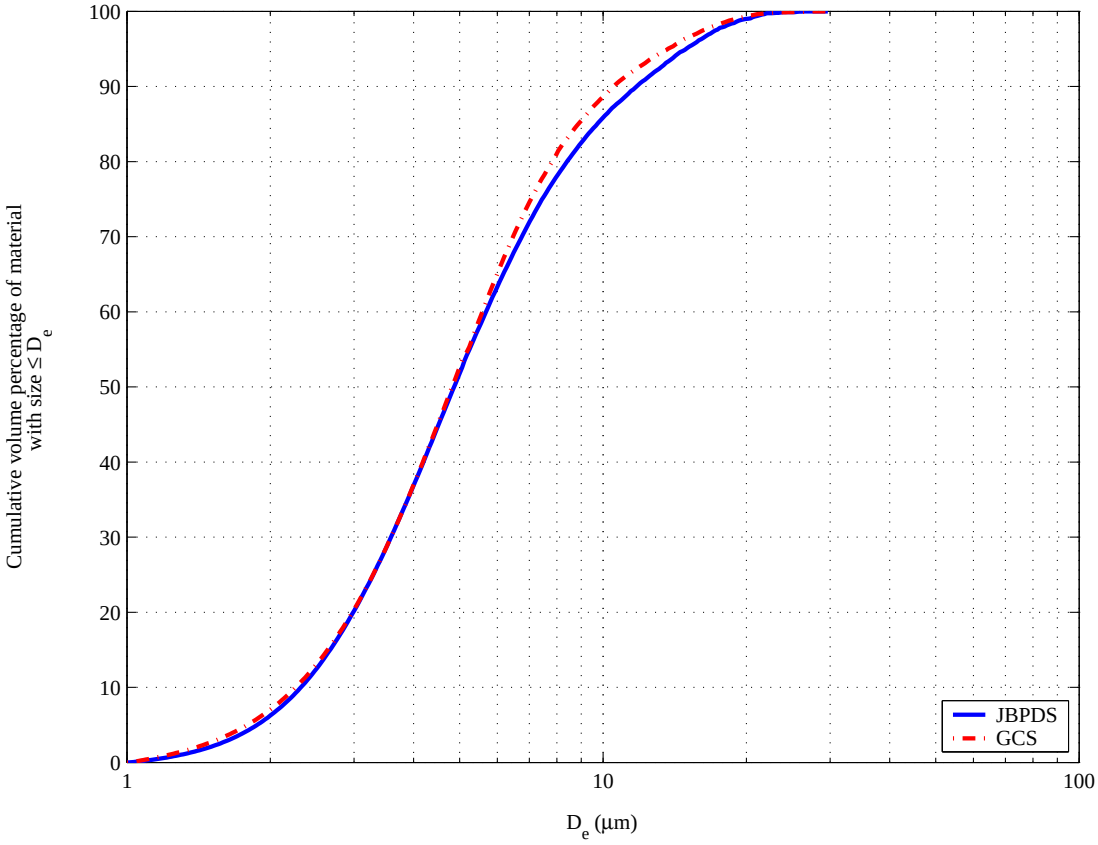

Figure 13. Cumulative size distribution of background (based on D_e) for the JBPDS and GSC cyclones.

13). If the incorrect size aperture tube is chosen, the size distribution will be an artifact of the detectable size range.

The size distribution of material the material captured by these two devices can be approximated by a log-normal distribution (Hinds 1999). The mass-median diameter, D_{mm}, for each device is approximately 4.8 μm. The geometric standard deviation, σ_g, for these two distributions is approximately 1.9. The curves in Figure 13 may be approximated by integrating the size distribution function, n_{p_v}:

$$n_{p_v} = \frac{1}{\sqrt{2\pi}\, D_p \, \ln \sigma_g} \exp\left(-\frac{(\ln D_p - \ln D_{mm})^2}{2(\ln \sigma_g)^2}\right) \qquad [17]$$

where D_p is a particle diameter and finding (for $\sigma_g = 1.9$ and $D_{mm} = 6.6$):

$$F_v(D_p) = 0.5 + 0.5\, erf(1.1 \ln D_p - 1.7) \quad [18]$$

The count median diameter may be calculated using the Hatch-Choate relation for different moments of a distribution. For conversion from the mass median diameter to the count median diameter, D_{nm}, the following equation is used:

$$D_{nm} = \frac{D_{mm}}{\exp(3 \ln^2 \sigma_g)} \quad [19]$$

Using Equation (19), D_{nm} is 1.4 μm. The data collected by the Coulter Counter indicates that the number median diameter is 1.8 to 1.9 μm. But, this number is influenced by the detectable size range of particles imposed by the aperture tube chosen.

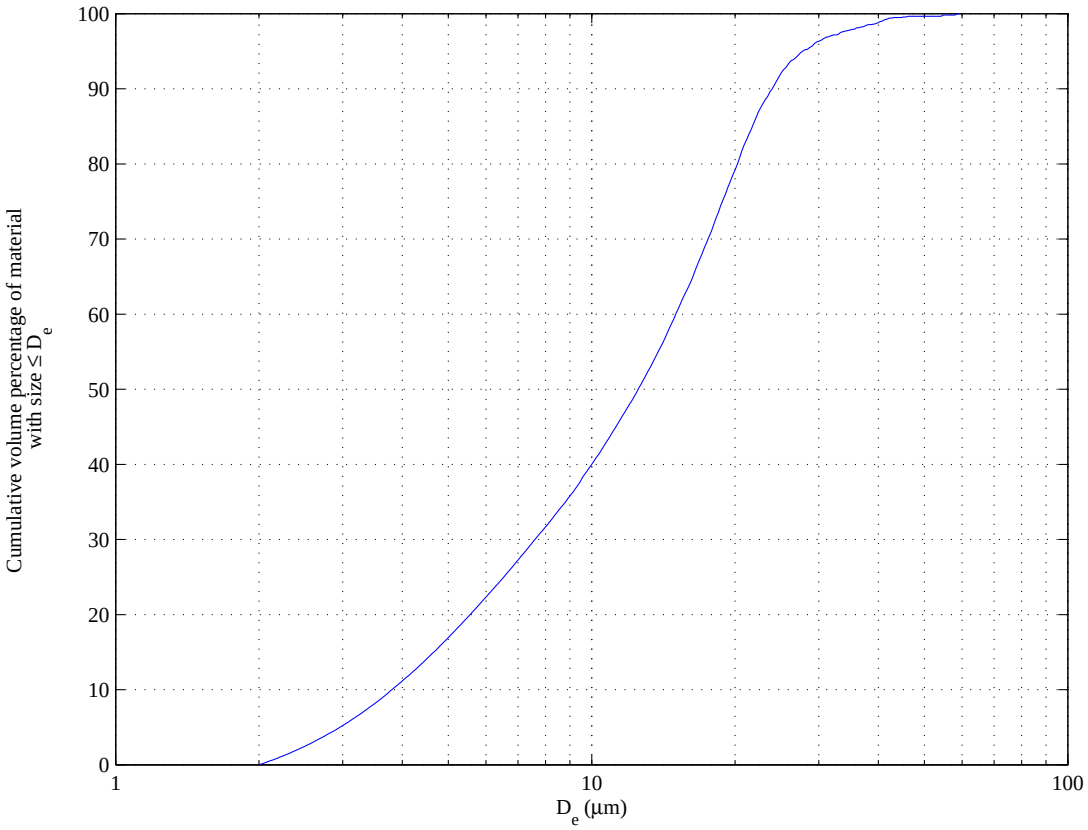

Figure 14. Cumulative size distribution (based on the D_e) of effluent background emissions. Note that the lower end of the distribution (around 2 μm) appears to be influenced by the lower detectable limit of the aperture tube.

For analysis of the filter data, the 50 μm aperture tube was not appropriate. Several different apertures were tried, and finally the 100 μm aperture was chosen. The results are plotted in Figure 14. From this figure, it is apparent that there was some influence on the size range imposed by the lower detectable limit of the aperture tube chosen. The mass median diameter of the distribution is 12.5 μm. Based on the data, the size distribution may not necessarily be approximated by a log-normal distribution. Therefore, σ_g has not been calculated.

Although background emission tests were conducted with the AHTS, no plot is presented in this study. A set of five tests was run using the AHTS to collect emissions. In each of the five tests, there was not enough particulate matter in the sample fluid to develop a size distribution using the Coulter Counter. The reason that the analysis was successful for the other devices and not the AHTS is related to the concentrating factor in each device. In the GCS and the JBPDS cyclones, 780 liters of sampled air is

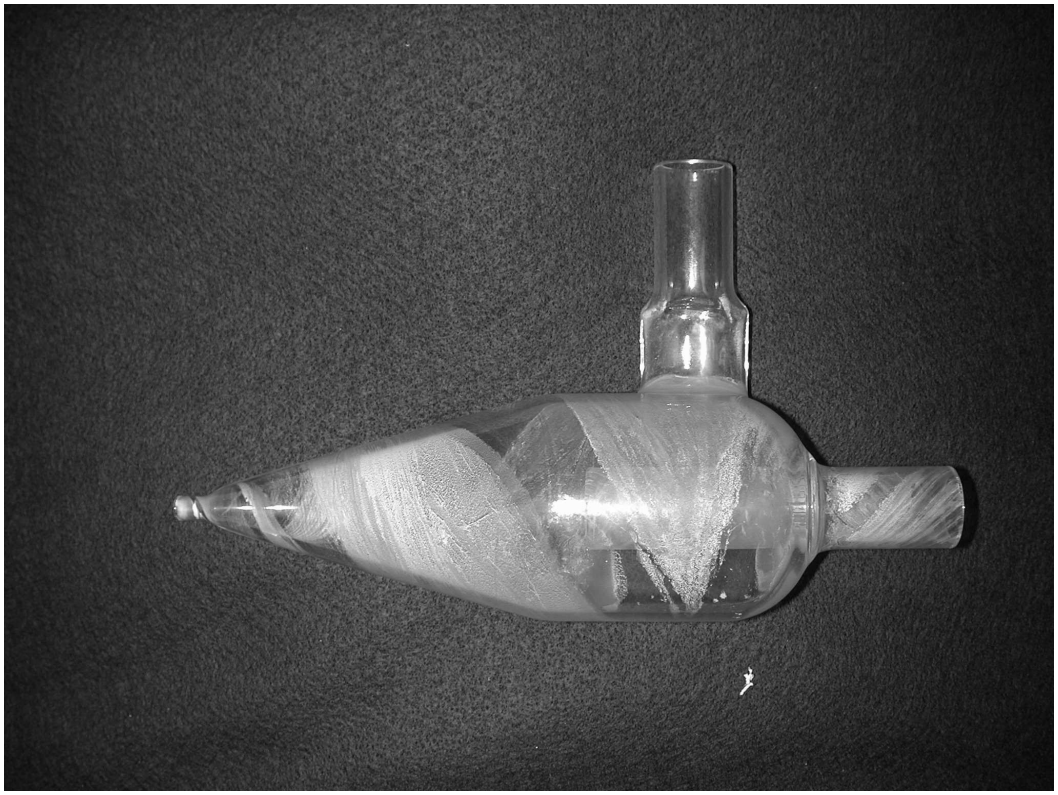

Figure 15. GCS after collection of background emissions.

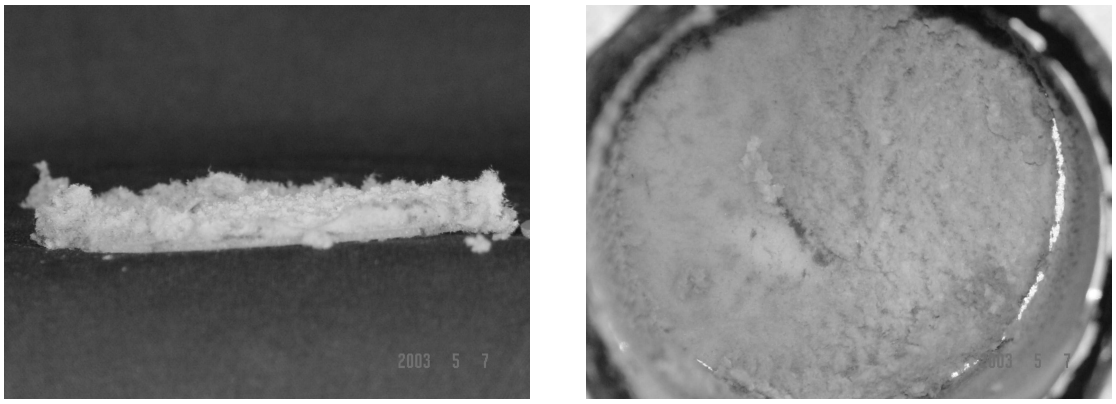

(a) (b)

Figure 16. Impactor surface after 7 hours of background emission collection. (a) Side view and (b) top view.

concentrated into ∼1 milliliter of fluid, whereas in the AHTS, only two liters of sampled air are concentrated into 1 milliliter of fluid. Based on this, the amount of particulate matter present in the cyclone fluids can be as high as 390 times that of the AHTS. This results in concentrations in the AHTS sample fluid that are not able to be analyzed by the Coulter Counter.

Figures 15 and 16 show the GCS and the impactor surface after a significant period of collection of background emissions. The JBPDS cyclone shows banding similar to the GCS after collection of background material. This buildup of material on the cyclone surfaces will most likely affect the collection of any microorganisms. The wetted surfaces in these devices tend to stay relatively free of debris, as can be seen from the photo of the GCS. However, not all of the liquid follows the banded path. Some fluid will move through the dirtier portions. Loss of bioaerosol particles to filtration by this deposited material may result, therefore reducing the collection efficiency of the device over time.

Another point of interest in the GCS is that the banding is not only present in the body of the cyclone, but also in the cyclone outlet. Upton et al. (1994) noticed a similar phenomenon when running tests. In the study cited, they attributed it to droplets contacting the vortex finder from the airstream and was accounted for by imperfections in the machining of the cyclone. This phenomenon occurred sporadically and affected

some cyclones tested more than others. In a CFD study by Griffiths and Boysan (1996), it was noted that there was some "leakage flow" of air entering the cyclone at the top of the inlet, swirling around the top to the outer-wall of the vortex finder, and turning rapidly to exit with the exhausted airstream; thereby short-circuiting the cyclone. In the tests conducted in this study, it was found that the solution, after impacting against the cyclone body wall, diverged from that the initial impaction point. Most of the fluid swirled around the cyclone body as expected and exited through the fluid outlet, but some flowed upward, spiraling around and eventually contacting the vortex finder. The fluid, after contact, swirled about the vortex finder and eventually exited through the cyclone outlet. As noted by Upton et al. (1994), the loss of liquid would result in the loss of sample and could also pose a potential health threat to those working around the sampling system. Also, the exhausted liquid might damage pumps, filters or meters. These two issues in this system are not of considerable concern because the air is treated by a HEPA filter before it ever reaches the system blower.

As noted above, the JBPDS cyclone also had developed bands due to incomplete wetting of the surface similar to those seen in the GCS (Figure 15). There was, however, another issue unique to this cyclone. At the initiation of the mail sorting process, the flow rate became unsteady, noticeably declining with each test period over which the flow rate was measured. This unstable flow rate may most likely be attributed to deposits in the gap between the cyclone wall and the liquid extraction sleeve at the outlet. To maintain enough vacuum so that liquid can be collected, this gap must be small. In the JBPDS cyclone design used in this study, the gap is approximately 0.1 mm. With high mass loading (i.e. with no trimming device upstream), this gap was blocked in every test after a period of 30 minutes of mail sorting. Reducing the mass loading using a trimming device reduced the occurrence of the blockage; but, the blockage continued intermittently.

As shown in Figure 16, the collection surface of the trimming impactor was overwhelmed after seven hours of operation. The debris collected on the surface had a height

of approximately 3 to 6 mm. At this height, the collected debris will begin to act as a filter. This in turn will reduce the D_{50} and affect the shape of the efficiency curve of the impactor.

Bioaerosol Releases

In the following sections, the results of the biological tests are presented. Due to the chaotic nature of the mail sorting process, there is high variability in the nature of a release of BG from an envelope during the mail sorting process. Due to this variability, the study is semi-quantitative, answering questions concerning the amount of bacteria released from the process only in terms of ranges of CFUs.

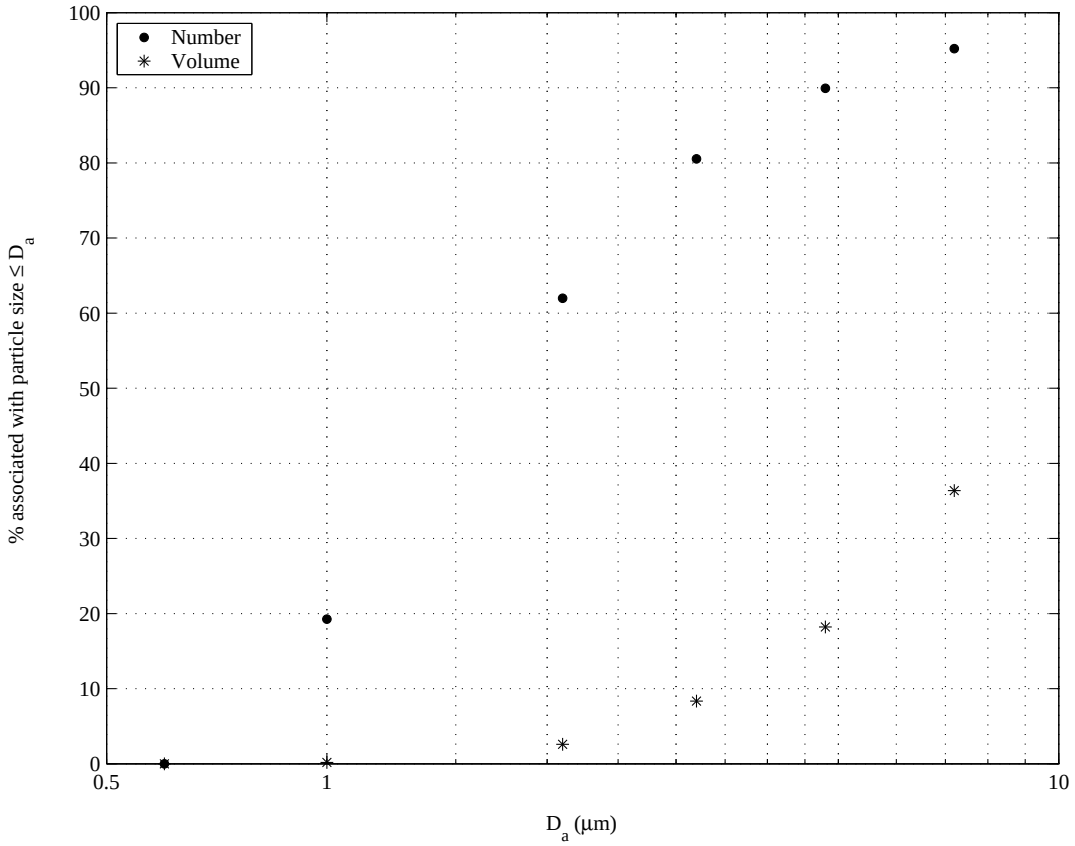

Figure 17. Size distribution of bacteria emitted from an envelope. (a) By number and (b) by volume.

Size Distribution

Figure 17 shows the cumulative size distribution of BG captured by the Anderson impactor in terms of both number and volume. The CFUs observed on the plates were adjusted using Equation (14) . The numbers shown in this table are the mean of 14 tests taken over two separate days. By number, less than 40% of the particles captured lie on or above the 3^{rd} stage. However, over 60% of the particle volume lies on the 1^{st} stage. Assuming that these particles on the 1^{st} stage are homogenous agglomerates, these results indicate that the majority of the spores captured are in clumps with an aerodynamic diameter greater than 7.2 μm, the D_a of the smallest particle captured by this stage. This result indicates that it is undesirable to set the D_{50} of any trimming device lower than 10 μm.

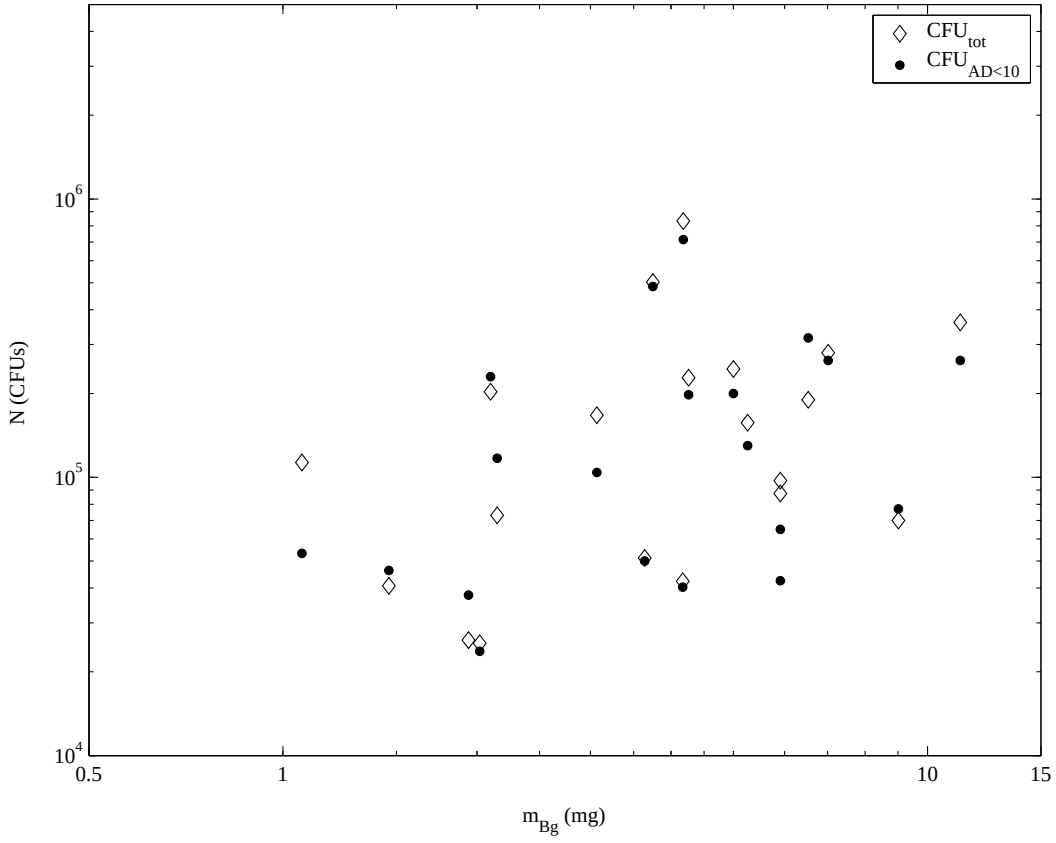

Figure 18. Number of CFUs captured using a gelatin filter for an envelope release.

Filter Capture

Data for bioaerosol captured on a gelatin filter is tabulated in Table A-4 and plotted here in Figure 18. From Table A-4, the average amount of bioaerosol particles with a D_a less than 10 μm is around 90%. However, the coefficient of variation, COV, is very large (35%). It is apparent that the mean was skewed by a few outliers in the data. This skewness may have been due to incorrectly metered flow or to an anomalous release. From this data, it can be inferred that the D_{50} of a trimming device may be set to 10 μm without significantly affecting the device output. However, due to the presence of outliers, further testing would be required to validate these results.

Device Capture

The results concerning the collection of BG released from an envelope are shown in the following figures. Each plot shows both the minimum and maximum responses as well as a line fitted to the data using a least-squares approach (Mandel 1964). The equation for the fitted line was found by taking the natural logarithm of the mass of BG, m_{BG}, and the number of CFUs, N, and using MATLAB's linear regression tool to fit the converted data to the equation $y = bx^a$. The equation for the line is given in the text as well as the coefficient of determination, r^2. The data was also tested to see whether N is a function of m_{BG}. In this case, the null hypothesis, H_o, is that N is not a function of m_{BG}. For each device, H_o is rejected if the probability, p, of observing the given results is less than the significance level, α. For each device, the threshold value used for the significance level was 0.05.

Data for each of the plots presented was collected over an extended period of time (several months). In the case of some of the earlier tests, the test time was not 5 minutes. In order to be able to present that data, the total number of CFUs observed was adjusted by a correction factor, C. This factor was based on data collected in system response

time tests, presented in a following section. The correction factor, C, is equivalent to:

$$C = \frac{1}{\%\ Response\ \ Expected} \qquad [20]$$

All data collected and adjusted is presented in Appendix A.

Collection data for the AHTS is shown in Figures 19(a) and (b). Using the reference setup in Figure 6, samples were collected concurrently with the GCS (except for in one set of tests, in which the JBPDS cyclone was used in the place of the GCS). The sample output of the AHTS and the GCS were compared to validate that each device was sampling correctly. In all tests, the collection trend of the AHTS matched that of the GCS despite the fact that the AHTS flow was not processed by a trimming device.

In Figure 19(a), the maximum number of CFUs recovered by the AHTS was approximately 10^5. This response occurred at 10.2 mg. However, this appears to be an anomaly. A similar response can be seen in Figure 20 for the GCS. From the data, it appears that the response is a full order of magnitude from what should be expected. However, as previously stated, a sample with the GCS was taken concurrently, and a similar response was noted for this release. If the AHTS data is extrapolated to determine the total num-

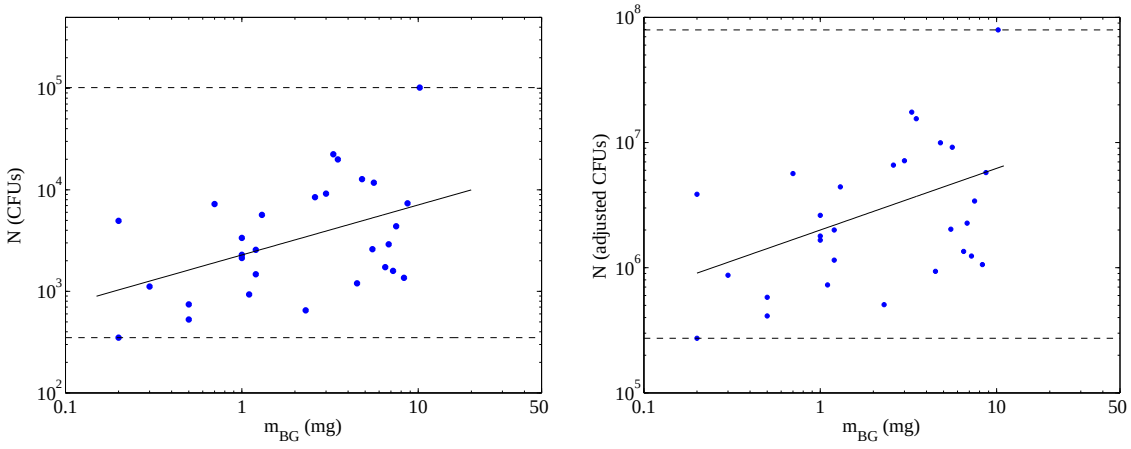

(a) (b)

Figure 19. Plotted data for a biological capture with the AHTS. (a) Actual number of CFUs captured, and (b) number of CFUs counted adjusted for a 780 L/min flow rate.

ber of CFUs for a 1 mg release, as shown in Figure 19(b), the expected number of CFUs captured by a device for a 1 mg release is approximately 2×10^6 CFUs.

For the fit, the coefficient a is 0.49 and the coefficient b is 2283.1. The coefficient of determination for this fit, r^2, is 0.21. Despite the low coefficient of determination, when tested, N is definitely a function of m_{BG} ($p = 0.01$).

The data collected for the GCS is plotted in Figure 20. For the fitted line and $a = 0.42$, $b = 5.47 \times 10^5$. For this fit, r^2 is 0.14. Similar to the AHTS, the correlation between N and m_{BG} is weak. The difference between the coefficient of determination of the GCS and that of the AHTS most likely arises from the difference in the number of tests run for each device and not from difference in collection efficiencies. At $p = 0.06$, it is questionable whether N is a function of m_{BG}.

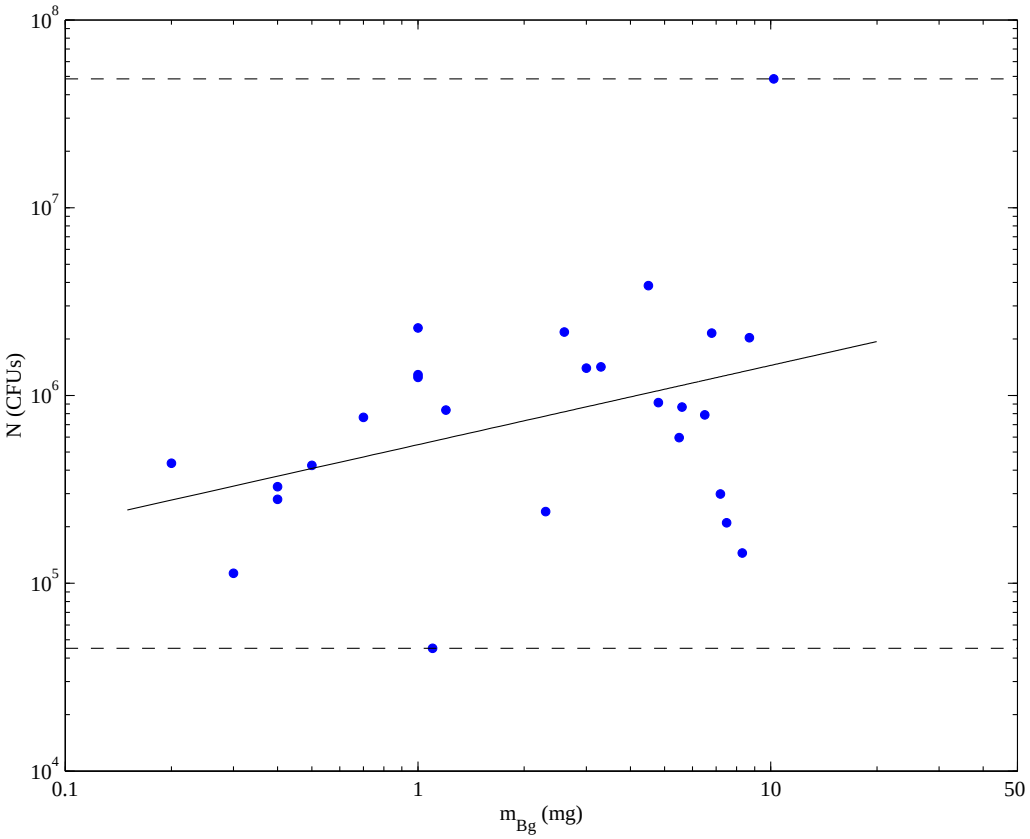

Figure 20. Plotted data for biological capture with the GCS.

In Figure 20, the maximum number of CFUs recovered by the GCS was 4.85×10^7 and occurred for a release involving a mass of BG of 10.2 mg. This is roughly half what would be expected given the extrapolated AHTS data in Figure 19(b). But, as previously noted concerning AHTS data, this maximum appears to be anomaly, far above what might be an expected result. The minimum response occurred during a release of 1.1 mg. For this release, 4.51×10^4 CFUs were recovered. This response was not noted in the AHTS, which ran concurrently with the GCS. Disregarding this low value at 1.1 mg, the average response of the GCS at approximately 1 mg is roughly half that expected given the extrapolated AHTS data in Figure 19(b).

Data concerning the JBPDS cyclone is plotted in Figure 21. For the fitted line, a is 0.15 and b is 3.05×10^5. For this line, r^2 is 0.05. Based on the coefficient of determination, this correlation is the poorest of the three device fits. For these tests, the maximum response for JBPDS cyclone was 2.24×10^6 CFUs corresponding to a mass of BG of 3.5 mg. The minimum response occurred at 0.3 mg and resulted in 8.08×10^4 CFUs. As expected from analyzing the exponent, a, the probability that H_o should be accepted is large ($p = 0.38$), therefore casting doubt on the assumption that N is a function of the mass of BG in the envelope.

The low r^2 value for the device fits may be accounted for in the scatter of the data. This scatter indicates that N is not exclusively a function of m_{BG}, if it is a function at all. The amount that is released may rely on many factors including the the amount of air in the envelope, the pressure exerted on the envelope, and the placement of the BG in the envelope. It is expected that for each device the number captured should be a function of the mass of BG in the envelope, however weak. Further investigation is required as to why there is question that this in not necessarily the case for both wetted-wall cyclones. In the case of the JBPDS cyclone, the obstruction of the fluid skimmer is most likely a factor.

Maximum and minimum responses along with the average response for a one mil-

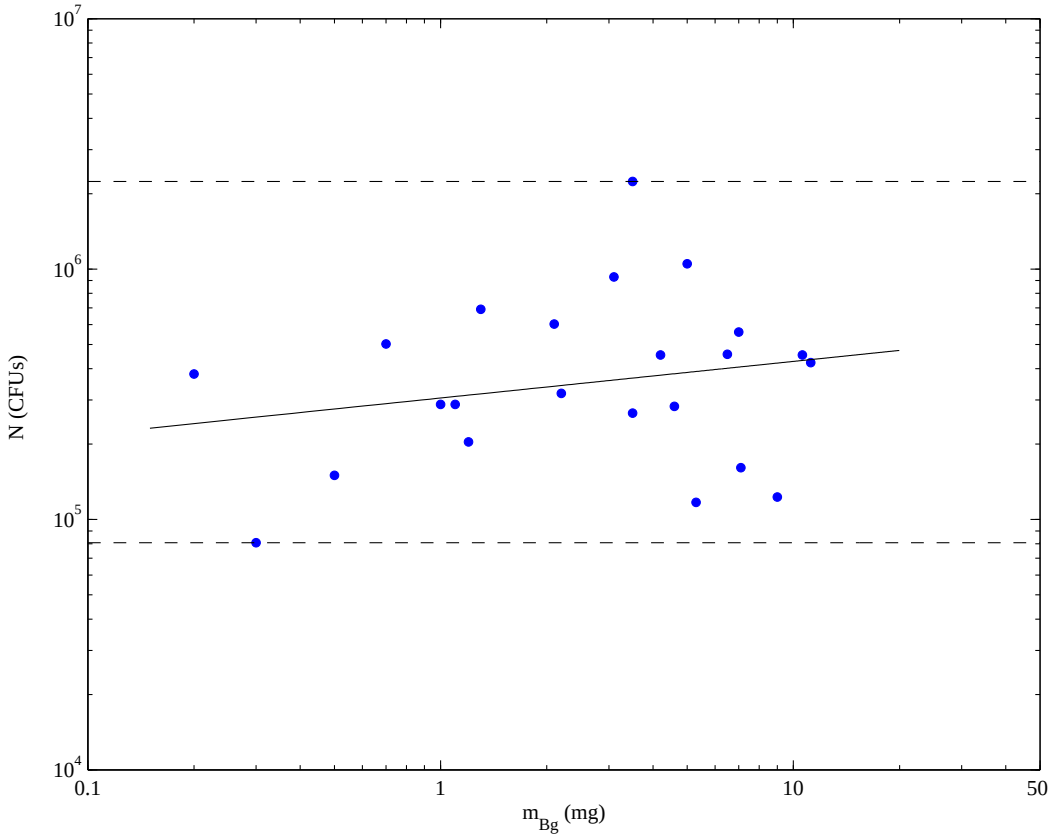

Figure 21. Plotted data for a biological capture with the JBPDS cyclone.

ligram release are summarized in Table 5. This table is provided to demonstrate the difference in collection results for the various devices. For this reason, the data shown for the AHTS is the extrapolated count of CFUs ($N \times 780$). When examining these tables, one must keep in mind that the flow sampled by the AHTS is untrimmed, whereas the main flow has an impactor which removes particles with a D_a less than 10 μm . However, using the filter data plotted in Figure 18, it can be assumed that only a small fraction (less than one tenth) of the CFUs are attributed to clumps with a D_a greater than 10 μm. The average response for a 1 mg release is an approximation and was found by averaging the response of each device for a 1 to 1.3 mg release. The anomalous minimum response of the GCS at 1.1 mg was not factored into the average for the GCS. At one milligram, the expected response (based on the extrapolated AHTS data) is one and a half times

Table 5. Summary of device responses with the mass of BG (mg) in parenthesis. For comparative purposes, the extrapolated number of CFUs is reported for the AHTS. Row two shows the average device response for a 1 mg release.

	AHTS (extrapolated)	GCS	JBPDS cyclone
N_{min} (m_{BG})	2.73×10^5 (0.2)	4.51×10^4 (1.1)	8.08×10^4 (0.3)
$N_{m_{BG}=1\ mg}$	2×10^6	1.3×10^6	3.7×10^5
N_{max} (m_{BG})	7.93×10^7 (10.2)	4.85×10^7 (10.2)	2.24×10^6 (3.5)

greater than the GCS response and five and a half times greater than the JBPDS cyclone response. Based on the most recent data collected, the expected average response is approximately 1.5 to 3 times greater than the GCS response. Due to the limited amount of samples taken concurrently with the JBPDS and the AHTS, no conclusion has been drawn concerning the relative JBPDS cyclone results.

System Response Time

Data for the system response time tests were taken over two days. The data collected is tabulated in Tables A-5 and A-6. For the GCS response time tests, samples were taken at one minute intervals for a total period of five minutes. From Figure 22(a), there is very little scatter in the data. On average, approximately 55% of the CFUs collected over a five minute interval are collected in the first minute.

The response time data for the JBPDS, shown in Figure 22(b), was taken at 30 second intervals for a total of 5 minutes. From Figure 22(b), on average, the majority of the response occurred within the first minute and a half. However, there is much scatter in the data. The reason that there is more scatter in the JBPDS cyclone data than the GCS most likely has to do with the shorter collection period. Also, obstruction of the skimmer gap in the JBPDS cyclone may have contributed to the high variation in the samples.

The traditional definition of the time constant, τ, of a system is defined as the period

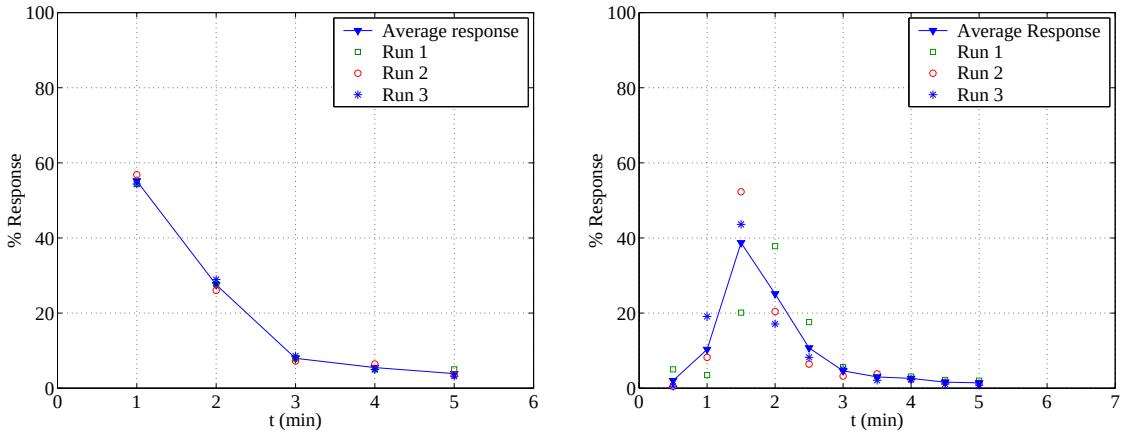

(a) (b)

Figure 22. Response time data for the wetted wall cyclones. (a) GCS response time, and (b) JBPDS cyclone response time.

required for the device to collect and deliver 63.2% of the steady state output in response to a step input (Holman 1966, p. 21). In this case, the traditional definition is not applicable because the input is impulsive. Therefore, for this system, τ is defined as the amount of time for the device to collect and deliver 63.2% of the total material for a five minute period in response to an impulse input (i.e. letter release). Given this definition, τ may be found via linear interpolation for each wetted wall cyclone. For the GCS, τ is 1.3 minutes; for the JBPDS cyclone, τ is 1.7 minutes.

SUMMARY AND CONCLUSIONS

This paper is the result of extensive testing performed on a system designed to collect biological particles (bioaerosols) emitted from a mail sorting machine. The aspiration efficiency of this system is nearly 100% at 780 L/min, the system flow rate. Particle deposition in the system is minimal. All particles are collected using one of two wetted-wall cyclones with a sample fluid output of $\sim$ 1 mL/min. At 780 L/min, the system should be able to collect particles larger than 1 μm, which is in the size range of a single BG spore.

Tests were conducted to characterize background emissions. Based on filter data, the mass emission rate is approximately 3.15 mg/min, with around two-thirds of the mass coming from particulate with a D_a less than 10 μm. Data from the Coulter Counter indicate that the volume equivalent mass median diameter was approximately 12.5 μm. However, this diameter may have been influenced by the lower detectable size limit of the aperture tube used. For the final collection devices, with a trimming impactor upstream (D_{50} = 10 μm), the volume equivalent mass median diameter of particles collected is 4.8 μm with a geometric standard deviation of approximately 1.8 or 1.9. No reliable data were produced for the size distribution of background material from the AHTS. The difference in mass median diameter of material in the main air flow and material captured by a device may be attributable to two causes. The first is the action of the trimming impactor. The second is that some of the larger material may permanently deposit on the walls of the cyclones. This deposition is clear in Figure 15.

Using an Anderson impactor, over 60% of the volume of biological particles collected was captured by the 1^{st} stage. On the top stages of the device, assuming homogenous agglomeration, a clump that results in a single colony may contain a large number of BG spores. Since the majority of the volume of material captured by the impactor is on the top stage, it is evident that the sampled size range not necessarily be limited to the

respirable size range. Further tests using gelatin filters seem to indicate that the majority of the bioaerosol clumps have an aerodynamic diameter less than 10 μm.

Two sampling cyclones were tested, the GCS and the JBPDS cyclone. On average, for a one milligram release, the GCS captures 3.5 times as many CFUs as the JBPDS. However, the expected number of CFUs released at one milligram is still 1.5 times that which is collected by the GCS. For a release of bioaerosol particles from an envelope, the system response time for the GCS is 1.3 minutes whereas the system response time for the JBPDS cyclone is 1.75 minutes.

The GCS appears to be more robust than the JBPDS cyclone. The gap in the skimmer of the JBPDS cyclone clogs intermittently requiring the system be taken apart and the cyclone cleaned. The GCS is also better characterized in terms of modelling and experimental analysis and is commonly used in other bioaerosol applications. Due to the robustness issues associated with the JBPDS cyclone and the slightly better performance of the GCS with respect to time and collection, this study indicates that the GCS is a reasonable choice for collection device of this system.

The system meets the requirements of the detectors that Siemens Dematic is considering. Testing is currently underway to determine potential background interference issues and integrated response times. Much of the research instrumentation used is being removed and a more robust design for the perforated plates is being introduced for these tests. Ultimately, an attempt will be made to draw a correlation between detector and collection system response. The detector response will be based on the output parameters of the devices and the collection system response will be evaluated using an appropriate counting technique.

One final note is required regarding the collection of reference samples. In this system, shrouded probes were chosen due to their excellent sampling characteristics in off-nominal conditions (McFarland et al. 1989). These probes were designed when the system was still in a conceptual phase. At the time of design, the estimated system flow rate was

1100 L/min and the dimensions of the duct in which the probes would reside were in flux. Towards the end of this study, the dimensions of the probes were re-examined and found to be incorrect for the sampling situation encountered here.

The shroud diameter for these probes is 31 mm and the probe inlet diameter is 8.6 mm. For a 28.3 L/min probe flow rate, the inlet velocity of the probe is 8.05 m/s. At 780 L/min, the free stream velocity in the duct is 1.26 m/s. Based on these numbers, the velocity within the shroud, u_o, is between 0.62 m/s and 1.26 m/s. Therefore, the ratio of the free stream velocity to the probe inlet velocity, u_o/U_p is between 0.08 and 0.16. The following equation may be used to find the aspiration efficiency of the probe operating

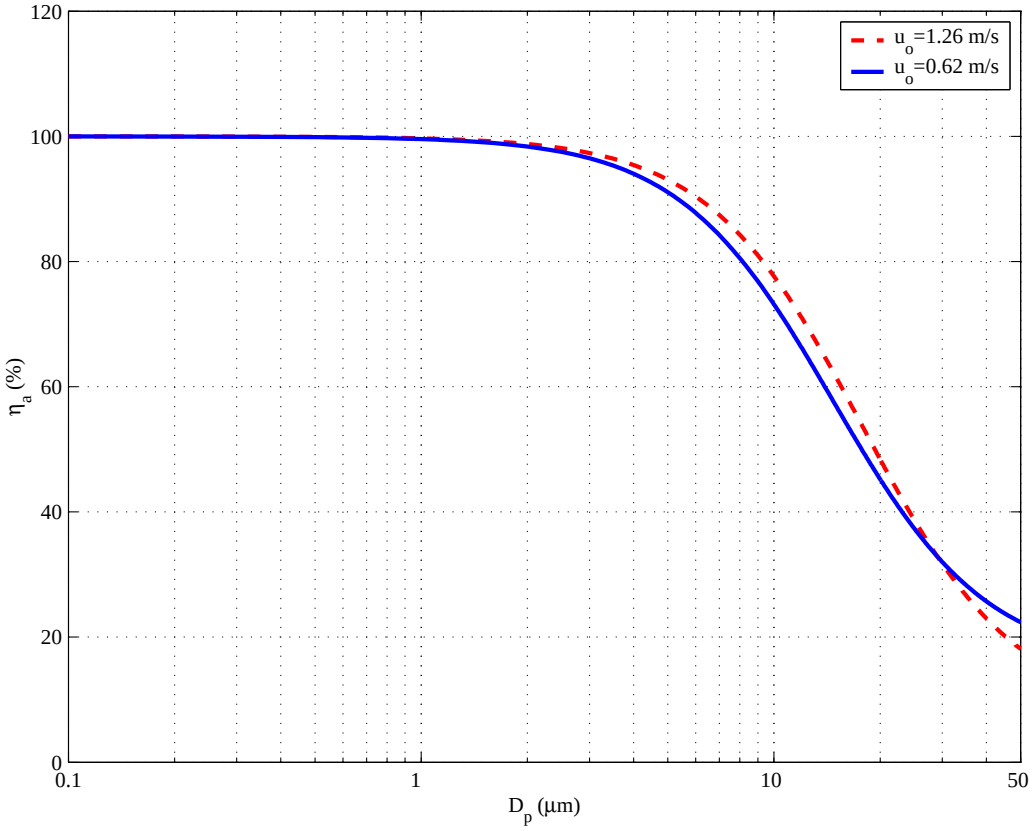

Figure 23. Shrouded probe aspiration efficiency for two different shroud velocities. The lower velocity lies outside the conditions presented in the use of Equation (21).

under super-isokinetic probe (Willeke and Baron 1993, p. 87):

$$\eta_a = 1 + \frac{(u_o/U_p - 1)}{1 + 0.506\,(u_o/U_p)^{1/2}/Stk} \qquad [21]$$

The Stokes number, Stk, is calculated using Equation (7) . In this case, the characteristic dimension, W, is the probe inlet diameter. Based on the above dimensions, η_a is plotted for both maximum and minimum possible shroud velocities in Figure 23. The limiting conditions for Equation (21) are $0.01 \leq Stk \leq 100$ and $0.1 \leq u_o/U_p \leq 10$. Despite this, the equation is plotted for the minimum velocity ratio and particle diameters with a Stk less than 0.01 ($D_p < 3.3$ μm for $u_{o,max}$ and $D_p < 4.7$ μm for $u_{o,min}$) for illustrative purposes.

From Figure 23, η_a is $\sim$ 75% for each shroud velocity at a D_a of 10 μm. For D_a greater than 10 μm, η_a declines steadily. It is apparent from these results that no matter the velocity, the aspiration efficiency of the probe will affect the collection results for most particle sizes of interest. Using these plots, some of the results of these tests may be corrected. However, the final result will be strictly qualitative and should be validated experimentally.

RECOMMENDATIONS FOR FUTURE WORK

For work to continue on this project, it is of principal concern that the reference samples that are taken be representative of the aerosol present in the system. To achieve this, a redesign of the probes is necessary. Due to the space limitations within the duct, it is recommended that probes designed for sampling be isokinetic, thin walled nozzles, as opposed to the shrouded probe. The probes should be designed for a flow rate of 28.3 L/min, since this is the operational flow rate of the Anderson impactor (Anderson 1958).

Another issue that will have to be addressed concerning this system is the trimming impactor. The current impactor requires cleaning within eight hours. In the postal environment, it is desirable to have parts that require less maintenance. Therefore, a study should be undertaken to more finely resolve the size distribution of the effluent aerosol according to D_a. Then, the impactor should be redesigned based on this data. The impactor should have a larger impaction surface area that requires less maintenance (i.e. multiple jets or a cascade of jets). An alternative to this is the use of a virtual impactor, which has no impaction surface.

In continuing the study of bioaerosols in relation to the post office environment, it is recommended that the student following up have a strong background in statistical analysis. Although this is very useful for all aerosol studies, it is especially useful for studies concerning bioaerosols. Due to the amount of scatter involved in all studies of bioaerosols, the statistical analysis of variance becomes crucial and is used in many studies.

Related to the topic of statistical analysis is a more fundamental study of the factors affecting the number of bioaerosol particles released from an envelope. Although the studies here suggest that the number of spores released is a function of the mass of BG in an envelope, it is apparent from the coefficient of determination that the number released is weakly correlated to the mass in the envelope. Ultimately, the number released will be a function of environmental conditions, the survival ratio of bacteria, the pressure applied

to an envelope, and others factors. These different factors should be identified and a function should be proposed such that:

$$N = N(RH, P_o, T_o, P_{applied}, SR, \ldots) \quad [22]$$

A linear regression approach should should be taken and variables found not to be statistically significant should be eliminated.

Before studies in the postal environment continue, biological collection efficiencies for each of the wetted wall cyclones should be established using the device configurations presented here in this study. When measuring the collection efficiency of the different cyclones, other counting methodologies should be considered. These methods should take into account total number of bacteria captured as opposed to just the viable number (performed in this study). Using spore stains or Gram stains, phase contrast microscopy, and some type of counting chamber (such as a Haemacytometer), researchers here may be able to determine more accurately collection efficiencies. Total count procedures should be adapted for all biological analysis.

A study should be undertaken to determine the size distribution of the spore powder as delivered to the ATL. A method should be developed such that the powder may be aerosolized while introducing a minimum amount of background particulate matter. This might be done using a high pressure jet of air to blast the powder from a surface. The resulting aerosol size distribution should then be measured using a device that can reliably measure aerodynamic particle size down to 0.8 μm. The tests should be conducted in a clean environment such as a biological safety cabinet.

REFERENCES

Anderson, A. (1958). New Sampler for the Collection, Sizing, and Enumeration of Viable Airborne Particles, *J. Bacteriol.* 23(76):471–484.

Avalone, E. A. and Baumeister, T., III, eds. (1996). *Marks' Standard Handbook for Mechanical Engineers*, McGraw Hill, New York, 10^{th} ed.

Black, R. (2002). Development of the Wet Walled Cyclone Collector for the Joint Biological Point Detection System, Presentation to the 2002 Scientific Conference on Obscuration and Aerosol Research, Edgewood, MD.

Breed, R., Murray, E., and Smith, N. (1957). *Bergey's Manual of Determinative Bacteriology*, The Williams and Wilkins Company, Philadelphia.

Centers for Disease Control and Prevention (2001a). Evaluation of *Bacillus anthracis* Contamination inside the Brentwood Mail Processing and Distribution Center – District of Columbia, October 2001, *MMWR* 50(50):1129–1133.

Centers for Disease Control and Prevention (2001b). Update: Investigation of Bioterrorism–Related Anthrax–Connecticut, 2001, *MMWR* 50(48):1077–1079.

Cooper, C. D. and Alley, F. (1994). *Air Pollution Control: A Design Approach*, Waveland Press, Prospect Heights, IL, 2^{nd} ed., ch. 4.

Cruickshank, R. (1960). *Mackie and McCartney's Handbook of Bacteriology: A Guide to Laboratory Diagnosis and Control of Infection*, E. & S. Livingstone Limited, Edinburgh.

Decker, H., Buchanan, L., Frisque, D., Miller, M., and Dahlgren, C. (1969). Advances in Large-Volume Air Sampling, *Contamination Control* 8:13–17.

Dull, P. M., Wilson, K. E., Kournikakis, B., Whitney, E. A., Boulet, C. A., Ho, J. Y. W., Ogston, J., Spence, M. R., McKenzie, M. M., Phelan, M. A., Popovic, T., and Ashford, D. (2002). *Bacillus anthracis* Aerosolization Associated with a Contaminated Mail Sorting Machine, *Emerging Infectious Diseases [serial online]* 8(10), available from URL: http://www.cdc.gov/ncidod/EID/vol8no10/02-0356.htm.

Golden, J., Rowe, C., Feldstein, M., Scruggs, S., Tender, L., and Ligler, F. (2002). *Array-Based Biosensor for Multianalyte Sensing*, Tech. rep., Center for Bio/Molecular Science and Engineering, Washington, DC.

Gong, H. (1996). Numerical Prediction of Shrouded Probe Sampling Performance: A Study of Subgrid Scale Models in Large Eddy Simulation, Ph.D. thesis, Texas A&M University, College Station.

Griffiths, W. and Boysan, F. (1996). Computational Fluid Dynamics (CFD) and the Empirical Modelling of the Performance of a Number of Cyclone Samplers, *J. Aerosol Sci.* 27(2):281–304.

Griffiths, W., Stewart, I., Futter, S., Upton, S., and Mark, D. (1997). The Development of Sampling Methods for the Assessment of Indoor Bioaerosols, *J. Aerosol Sci.* 28(3):437–457.

Griffiths, W., Stewart, I., Reading, A., and Futter, S. (1996). Effect of Aerosolisation, Growth Phase and Residence Time in Spray and Collection Fluids on the Culturability of Cells and Spores, *J. Aerosol Sci.* 27(5):803–820.

Henis, Y., ed. (1987). *Survival and Dormancy of Microorganisms*, John Wiley & Sons, New York.

Henningson, E., Lundquist, M., Larsson, E., Sandström, G., and Forsman, M. (1997). A Comparative Study of Different Methods to Determine the Total Number and the Survival Ratio of Bacteria in Aerobiological Samples, *J. Aerosol Sci.* 28(3):459–469.

Hinds, W. C. (1999). *Aerosol Technology: Properties, Behvior, and Measurement of Airborne Particles*, John Wiley & Sons, New York, 2^{nd} ed.

Holman, J. (1966). *Experimental Methods for Engineers*, McGraw-Hill Book Co., New York.

Iozia, D. and Leith, D. (1989). Effect of Cyclone Dimensions on Gas Flow Pattern and Collection Efficiency, *Aerosol Sci.Technol.* 10:491–500.

Iozia, D. and Leith, D. (1990). The Logisitic Function and Cyclone Fractional Efficiency,

Aerosol Sci.Technol. 12:598–606.

Kournikakis, B., Armour, S., Boulet, C., Spence, C., and Parsons, B. (2001). *Risk Assessment of Anthrax Threat Letters*, Tech. Rep. DRES TR-2001-048, Defense Research Establishment Suffield, Canada.

Macher, J. (1989). Positive-Hole Correlation of Multiple-Jet Impactors for Collecting Viable Microorganisms, *Am. Ind. Hyg. Assoc. J.* 50(11):561–568.

Macher, J., ed. (1999). *Bioaerosols: Assessment and Control*, American Conference of Governmental Industrial Hygienists, Cincinnati, OH.

Mandel, J. (1964). *The Statistical Analysis of Experimental Data*, Dover Publications, New York.

Marple, V. A. and Liu, B. Y. (1974). Characteristics of Laminar Jet Impactors, *Environ. Sci. Technol.* 8(7):648–654.

McFarland, A., Anand, N., Ortiz, C., Gupta, R., Chandra, S., and McManigle, A. (1999). A Generic Mixing System for Achieving Conditions Suitable for Single Point Representative Effluent Air Sampling, *Health Physics* 76(1):17–26.

McFarland, A., Ortiz, C., Moore, M., R.E. DeOtte, J., and Somasundaram, S. (1989). A Shrouded Aerosol Sampling Probe, *Environ. Sci. Technol.* 23(12):1487–1491.

Moore, M. and McFarland, A. (1993). Performance Modeling of a Single-Inlet Aerosol Sampling Cyclones, *Environ. Sci. Technol.* 27(9):1842–1848.

Ortiz, C. (2002). Personal communication, Aerosol Technology Laboratory, Texas A&M University, College Station.

Peters, C. and Hartley, D. (2002). Anthrax Inahalation and Lethal Human Infection, *The Lancet* 359(9307).

Peters, C., Spertzl, R., and Patrick, W., III (2002). Aerosol Technology and Biological Weapons, In *Biological Threats and Terrorism: Assessing the Science and Response Capabilities*, S. L. Knobler, A. MahMoud, and L. A. Pray, eds., National Academy Press, Washington, DC.

Phan, H. N. (2002). Aerosol-to-Hydrosol Transfer Stages for use in Bioaerosol Sampling, Master's thesis, Texas A&M University, College Station.

Prescott, L. M., Harley, J. P., and Klein, D. A. (1996). *Microbiology*, Wm. C. Brown Publishers, Dubuque, IA, 3^{rd} ed.

Quian, Y., Willeke, K., Grinshpun, S., and Donnelly, J. (1997). Performance of N95 Respirators: Reaerosolization of Bacteria and Solid Particles, *Am. Ind. Hyg. Assoc. J.* 58:876–880.

Rao, A. and Whitby, K. (1978). Non-Ideal Collection Characteristics of Inertial Impactors – I. Single Stage Impactors and Solid Particles, *J. Aerosol Sci.* 9:77–86.

Riehl, J., Dileep, V., Anand, N., and McFarland, A. (1996). *DEPOSITION 4.0: An Illustrated User's Guide*, Tech. Rep. 8836/07/96, Aerosol Technology Laboratory, Texas A&M Univeristy, College Station.

Upton, S., Mark, D., Douglass, E., Hall, D., and Griffiths, W. (1994). A Wind Tunnel Evaluation of the Sampling Efficiencies of Three Bioaerosol Samplers, *J. Aerosol Sci.* 25:1493–1501.

U.S. Environmental Protection Agency (2003). *40 CFR 60: Appendix A, Method 1 – Sample and Velocity Traverses for Stationary Sources*, Office of Federal Register National Archives and Records Administration, Washington, DC.

Wark, K., Jr (1988). *Thermodynamics*, McGraw Hill, New York, 5^{th} ed.

Weis, C. P., Intrepido, A. J., Miller, A. K., Cowin, P. G., Durno, M. A., Gebhardt, J. S., and Bull, R. (2002). Secondary Aerosolization of Viable *Bacillus anthracis* Spores in a Contaminated US Senate Office, *JAMA* 288(22):2853–2858.

White, F. M. (1999). *Fluid Mechanics*, WCB/McGraw-Hill, Boston, 4^{th} ed.

Willeke, K. and Baron, P. A., eds. (1993). *Aerosol Measurement: Principles, Techniques, and Applications*, Van Nostrand Reinhold, New York.

APPENDIX A

TABULATED BIOLOGICAL DATA

The following tables contain the data used to generate many of the plots concerning the biological data. They are provided here so that future researchers may analyze the data themselves. The intention of the presentation of this data is to provide insight into the collection and manipulation of the data.

The first three tables represent the material captured by a device. In these tables, V_o refers to the volume of fluid collected by the sampler, V_p is the volume plated, $\bar{n}$ is the average number of CFUs counted for a sample, the COV is the coefficient of variation for the sample, N is the total number of CFUs calculated using Equation (15) , and N_a is the number of CFUs adjusted for differences in collection time using Equation (20) . The COV may be calculated using:

$$COV = \frac{s}{\bar{n}} \qquad [A.1]$$

where s is the sample standard deviation Mandel (1964). In instances where the COV is blank, $\bar{n}$ is actually the result of one plate.

The fourth table presents the samples collected using the gelatin filters. These tables simply list the numbers plated for both the total sample taken and the sample taken processed by the cyclone (for D_a less than 10 μm). The final column presents the percentage with a D_a less than 10 μm.

The final two tables represent the data collected to ascertain the response time of the system in connection with each of the two wetted-wall cyclones. These tables are similar to the previous tables for device collection, but, these tables contain a column for the test time and the percent response. The percent response in this table is calculated as the number of CFUs counted for that particular period over the total number of CFUs summed over all of the periods.

Table A-1. AHTS Data.

m_{BG} (mg)	V_o (mL)	V_p (mL)	DF	$\bar{n}$ (CFUs)	COV (%)	N (CFUs)	N_a (CFUs)
0.5	1.5	0.1	1	32	1.82%	475	528
0.2	1.5	0.1	1	21	26.51%	315	350
1.0	1.5	0.1	1	137	34.59%	2060	2289
1.0	1.5	0.1	1	128	23.33%	1920	2133
0.3	2	0.1	1	53	21.3%	1060	1116
0.5	2	0.1	1	35	28.9%	707	744
0.2	2	0.1	1	235	6.0%	4700	4947
0.7	2	0.1	1	344	4.3%	6887	7249
1.0	2	0.1	1	160	9.2%	3190	3358
1.2	2	0.1	1	70	10.0%	1400	1474
1.3	2	0.1	1	269	6.5%	5380	5663
3.5	2	0.1	10	95	18.5%	18933	19930
1.2	2.5	0.1	2	51	11.41%	2567	
1.1	2.5	0.1	2	19	6.19%	933	
2.3	2.5	0.1	1	26	23.40%	650	
2.6	2.5	0.1	2	169	10.17%	8467	
3.0	2.5	0.1	10	37	20.47%	9167	
3.3	2.5	0.1	10	90	10.54%	22417	
4.5	2.5	0.1	1	48	9.55%	1200	
4.8	2.5	0.1	10	51	20.38%	12750	
5.5	2.5	0.1	1	104	12.72%	2600	
5.6	2.5	0.1	10	47	2.13%	11750	
6.5	2.5	0.1	1	69	21.84%	1733	
6.8	2.5	0.1	1	116	5.53%	2908	
8.7	2.5	0.1	1	295	1.41%	7367	
10.2	2.5	0.1	100	41	3.76%	101667	
7.2		0.1	1	64	14.25%	1592	
7.5		0.04	1	70	0.00%	4375	
8.3		0.1	1	54	22.49%	1358	

Table A-2. GCS Data.

m_{BG} (mg)	V_o (mL)	V_p (mL)	DF	$\bar{n}$ (CFUs)	COV (%)	N (CFUs$\times 10^5$)	N_a (CFUs$\times 10^5$)
0.5	2.5	0.1	100	153	16	3.83	4.25
0.2	2.5	0.1	100	157	17	3.93	4.36
0.7	2.3	0.1	100	306	3	6.89	7.65
1.0	2.3	0.1	1000	91	–	20.6	22.9
1.0	2.5	0.1	100	465	7	11.6	12.9
0.4	1.8	0.1	100	140	42	2.52	2.80
7.2	5.0	0.1	20	299	17.05	2.99	
7.5	5.3	0.1	100	40	21.79	2.10	
8.3	5.0	0.1	20	145	13.03	1.45	
6.5	5.5	0.1	100	143	1.07	7.88	
6.8	5.0	0.025	100	108	3.29	21.5	
8.7	5.8	0.1	1000	35	12.45	20.3	
10.2	5.0	0.1	10000	97	18.90	485	
1.2	5.5	0.1	100	152	5.39	8.36	
1.1	5.2	0.1	100	9	17.63	0.451	
2.3	5.2	0.1	100	46	8.99	2.41	
2.6	5.0	0.1	1000	44	9.26	21.8	
3.0	5.5	0.1	100	254	2.17	14.0	
3.3	5.5	0.1	100	257	2.97	14.2	
4.5	5.5	0.1	1000	70	13.63	38.5	
4.8	5.0	0.1	1000	18	38.31	9.17	
5.5	5.0	0.1	20	597	0.97	5.97	
5.6	5.0	0.1	1000	17	12.01	8.67	

Table A-3. JBPDS Cyclone Data.

m_{BG} (mg)	V_o (mL)	V_p (mL)	DF	$\bar{n}$ (CFUs)	COV (%)	N (CFUs$\times 10^5$)	N_a (CFUs$\times 10^5$)
6.5	5	0.1	100	91.33	46.59%	4.57	
7.0	5	0.1	100	112.00	18.81%	5.60	
9.0	5	0.1	100	24.67	18.72%	1.23	
11.2	5	0.1	100	84.67	24.39%	4.23	
2.1	5.2	0.1	100	116	37.96%	6.03	
3.5	5.4	0.1	100	49	19.48%	2.66	
4.6	5	0.1	100	57	7.35%	2.83	
5.3	4.8	0.1	100	24	24.08%	1.17	
7.1	5.5	0.1	100	29	50.26%	1.61	
10.6	5.8	0.1	100	78	21.75%	4.54	
1.1	5.5	0.1	100	52	12.72%	2.88	
2.2	5.2	0.04	10	245	–	3.19	
3.1	5.0	0.1	100	186	3.53%	9.30	
4.2	4.8	0.1	200	47	18.94%	4.54	
5.0	5.5	0.1	100	191	11.76%	10.5	
0.3	4.8	0.1	100	16	31.1%	0.768	0.808
0.5	4.5	0.1	100	32	19.8%	1.43	1.50
0.2	5	0.1	100	72	32.2%	3.62	3.81
0.7	5	0.1	100	95	49.6%	4.77	5.02
1.0	5	0.1	100	55	37.6%	2.74	2.88
1.2	5	0.1	100	39	25.7%	1.94	2.04
1.3	5	0.1	100	131	7.3%	6.57	6.91
3.5	5	0.1	200	213	5.5%	21.3	22.4

Table A-4. Filter data.

m_{Bg} (mg)	N_{tot} (CFUs$\times 10^4$)	$N_{D_a<10}$ (CFUs$\times 10^4$)	$\% < 10$
1.46	4.07	4.63	113.93
3.75	50.3	48.5	96.36
3.64	5.13	5.00	97.40
4.17	4.23	4.03	95.28
1.94	2.60	3.77	144.87
2.02	2.53	2.37	93.42
5.91	9.73	4.25	43.66
5.91	8.75	6.50	74.29
4.26	22.8	19.8	86.84
1.07	11.3	5.33	47.41
2.15	7.30	11.7	160.73
3.07	16.7	10.4	62.15
4.18	83.3	71.5	85.89
5	24.5	20.0	81.63
2.1	20.3	23.0	113.11
5.26	15.7	13.0	82.98
6.53	19.0	31.7	166.67
7.01	28.0	26.3	94.05
9.01	7.00	7.70	110.00
11.24	36.0	26.3	73.15
Average			96.19
COV			33.89%

Table A-5. GCS response time data.

t (min)	V_o (μL)	V_p (μL)	DF	$\bar{n}$ (CFUs)	COV (%)	N (CFUs$\times 10^3$)	% Response
1	1000	100	100	62	8.05	61.5	54.34
2	1000	100	100	31	30.33	31.3	27.69
3	1000	100	100	9	11.11	9.00	7.95
4	1000	100	100	6	10.19	5.67	5.01
5	1000	100	100	6	50.94	5.67	5.01
1	1000	100	100	186	2.66	186	56.84
2	1000	100	100	85	15.02	85.0	26.02
3	1000	100	100	24	17.08	23.7	7.24
4	1000	100	100	21	25.20	21.0	6.43
5	1000	100	100	11	28.36	11.3	3.47
1	1000	100	100	679	–	679	54.35
2	1000	100	100	361	3.46	361	28.90
3	1000	100	100	107	6.61	107	8.59
4	1000	100	100	62	14.82	62.3	4.99
5	1000	100	100	40	12.94	39.7	3.18

Table A-6. JBPDS cyclone response time data.

t (min)	V_o (μL)	V_p (μL)	DF	$\bar{n}$ (CFUs)	COV (%)	N (CFUs$\times 10^3$)	% Response
0.5	500	100	10	95	39.46	4.73	5.05
1.0	500	100	10	66	34.95	3.30	3.53
1.5	500	100	100	38	44.53	18.8	20.13
2.0	500	100	100	71	28.60	35.3	37.76
2.5	500	70	10	230	6.49	16.4	17.56
3.0	500	100	10	104	1.67	5.2	5.56
3.5	500	100	10	59	17.86	2.95	3.15
4.0	500	100	10	57	19.45	2.87	3.06
4.5	500	100	10	41	9.76	2.05	2.19
5.0	600	100	10	32	4.20	1.89	2.02
0.5	400	40	1	177	5.98	1.78	0.52
1.0	500	40	10	224	24.09	28.0	8.18
1.5	450	100	100	397	16.82	179	52.25
2.0	450	100	100	155	34.35	69.9	20.45
2.5	450	100	100	48	48.62	21.8	6.36
3.0	450	100	100	24	21.09	11.0	3.20
3.5	450	80	10	231	7.58	13.0	3.80
4.0	450	100	10	177	12.35	7.96	2.33
4.5	450	100	10	122	5.73	5.50	1.61
5.0	450	100	10	100	34.42	4.48	1.31
0.5	500	100	10	46	26.64	2.32	0.51
1.0	500	100	100	175	2.29	87.5	19.11
1.5	500	100	100	399	3.6	200	43.61
2.0	500	100	100	156	8.96	78.2	17.07
2.5	500	40	10	302	21.85	37.7	8.24
3.0	500	40	10	188	13.04	23.5	5.13
3.5	500	100	10	193	9.23	9.63	2.10
4.0	500	100	10	215	9.34	10.8	2.35
4.5	500	100	10	97	8.30	4.87	1.06
5.0	500	100	10	74	27.78	3.72	0.81

APPENDIX B

THE VENTURI METER

This section is intended for future users of the system. The flow rate of this system is monitored using a venturi meter. For this particular meter, the inlet diameter, D, is 50.8 mm and the throat diameter is, d, is 24.9 mm. For this particular meter, the parameters for calculating the flow rate are the flow coefficient, C_f (0.849) and the area ratio, β (0.4907). To calculate the flow rate, the following function is used:

$$Q_s = \frac{C_f\, A_2}{\sqrt{1-(d/D)^4}} \sqrt{\frac{2\,\Delta P_{vm}}{\rho}} \qquad \text{[B.1]}$$

In this case, A_2 refers to the area of the meter throat, ΔP_{vm} refers to the differential pressure across the meter, and ρ refers to the density of the metered gas at the inlet of the venturi meter. In Figure B-1, the flow rate as a function of differential pressure is plotted for three different inlet air densities. The second density represents the JBPDS cyclone standard operating condition and the third density represents the GCS standard operating cyclone.

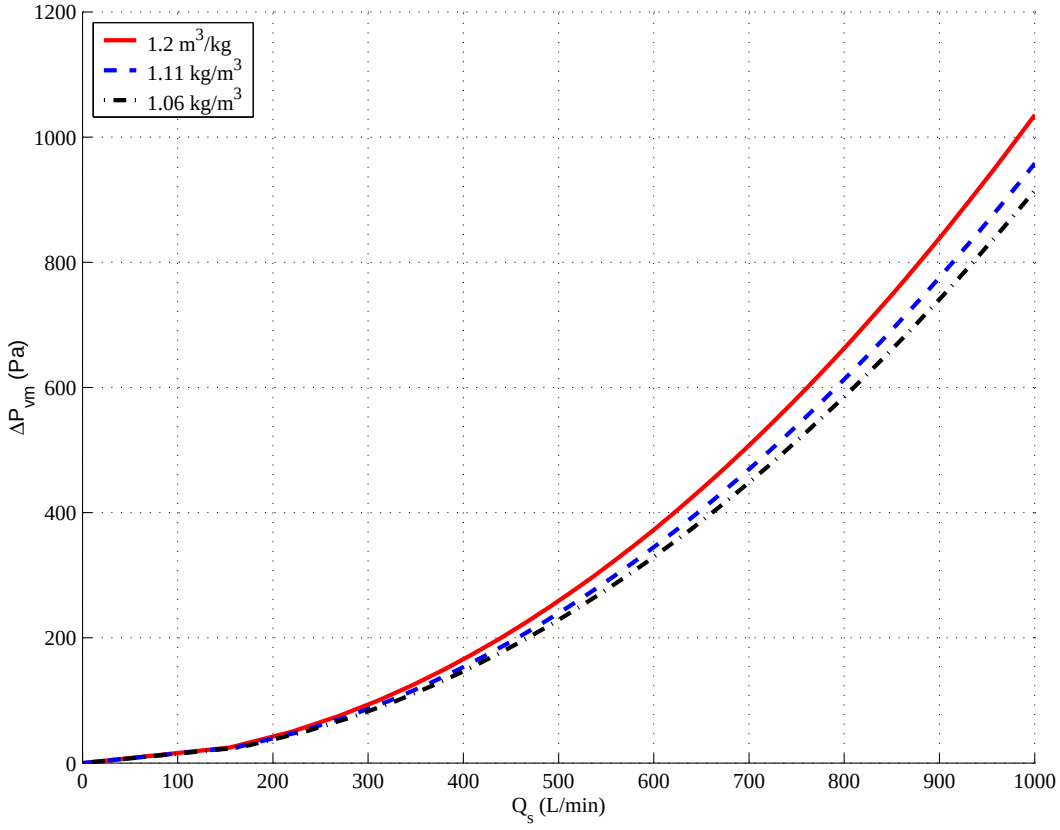

Figure B-1. Differential pressure versus flow rate for the venturi meter used by this system. The three different densities represent different operating conditions of the venturi meter.

VITA

Name:		Mathews Sears Richardson
Permanent Address:		4051 Tartan Houston, TX 77025
Education:		M.S. Mechanical Engineering August 2003 Texas A&M University College Station, TX
		B.S. Mechanical Engineering May 1999 University of Texas Austin, TX
Work Experience:	January 2002 to present	Graduate Research Assistant Aerosol Technology Laboratory Department of Mechanical Engineering Texas A&M University College Station, TX
	August 2002 to January 2001	Graduate Teaching Assistant Department of Mechanical Engineering Texas A&M University College Station, TX
	October 1999 to July 2001	Research Associate Booz, Allen and Hamilton Houston, TX